Seasonal Investigation of Ultrafine Particle Composition in an Eastern Amazonian Rainforest

Adam E. Thomas[1], Hayley S. Glicker[1], Alex B. Guenther[2], Roger Seco[3], Oscar Vega Bustillos[4], Julio Tota[5], Rodrigo A. F. Souza[6], and James N. Smith[1]

[1]Department of Chemistry, University of California, Irvine, USA
[2]Department of Earth System Science, University of California, Irvine
[3]Institute of Environmental Assessment and Water Research (IDAEA-CSIC), Barcelona, Catalonia, Spain
[4]Instituto de Pesquisas Energéticas e Nucleares, Cidade Universitaria, São Paulo, Brazil
[5]Universidade Federal do Oeste do Pará, Santarém, Brazil
[6]Escola Superior de Tecnologia, Universidade do Estado do Amazonas, Manaus, Brazil

Correspondence: James N. Smith (jimsmith@uci.edu)

1   Abstract

Reports on the composition of ultrafine (<100 nm in diameter) particles in the Amazon are scarce, due in part to the fact that new particle formation has rarely been observed near ground level. Ultrafine particles near the surface have nevertheless been observed, leaving open questions regarding the sources and chemistry of their formation and growth, particularly as these vary

5   across seasons. Here we present measurements on the composition of ultrafine particles collected in the Tapajós National Forest (2.857° S, 54.959° W) during three different seasonal periods: 10 - 30 September 2016 (SEP), 18 November - 23 December 2016 (DEC), and 22 May - 21 June 2017 (JUN). Size-selected (5 - 70 nm) particles were collected daily (22 h) using an offline sampler. Samples collected during the three time periods were compiled and analyzed using liquid chromatography coupled to Orbitrap high resolution mass spectrometry. Our findings suggest a sustained influence of isoprene organosulfate chemistry on

10   ultrafine particles in the different periods. We present chemical evidence that biological spore fragmentation impacted ultrafine particle composition during the late wet season (JUN), while chemical markers for biomass burning and secondary chemistry peaked during the dry season (SEP, DEC). Higher oxidation states and degrees of unsaturation were observed for organics in the dry season (SEP, DEC), suggesting greater extents of aerosol aging. Finally, applying a volatility parameterization to the observed compounds suggests organic sulfur species are likely key drivers of new particle growth in the region due to their low

15   volatility compared to other species.

2   Introduction

Ultrafine (<100 nm in diameter) aerosol particles (UAPs) are ubiquitous in the atmosphere, representing the largest fraction of ambient aerosol loading by number (Seinfeld and Pandis, 2006). Inhalation of these these particles are linked to adverse health effects in many different parts of the human body, as they are small enough to infiltrate deep into lung tissue, enter the

20 bloodstream, and cross the blood-brain barrier(Calderón-Garcidueñas and Ayala, 2022; Li et al., 2021; Nassan et al., 2021; Allen et al., 2017). Ultrafine particles can form in the atmosphere from the condensation of low volatility gases in a process known as new particle formation (NPF), considered to be the dominant emission pathway of new particles in the atmosphere (Dunne et al., 2016). Though too small themselves to interact with sunlight at most wavelengths, newly formed particles serve as a significant source of larger particles that can scatter or absorb incident solar radiation, directly impacting climate. In

25 addition, particles formed by NPF are estimated to contribute up to 50% of global cloud condensation nuclei (CCN), particles that can uptake water and serve as seeds for cloud droplets (Gordon et al., 2017; Westervelt et al., 2013; Merikanto et al., 2009; Wang and Penner, 2009). Another study has suggested that UAPs themselves may directly impact cloud formation and drive precipitation over the Amazon basin and other pristine areas by increasing the convective intensity of deep convective clouds (Fan et al., 2018), though this is still an area of active research (Varble et al., 2023). Critical to understanding UAP formation

30 as well as their impacts on human health and climate is information on their distribution and chemical composition as observed in different environments.

Although known for its pristine air quality (Andreae et al., 2004), the Amazon basin nevertheless serves as one of our planet's largest aerosol reservoirs thanks in part to its large area and abundant biogenic volatile organic compound (BVOC) emissions (Guenther et al., 2012), directly impacting the global CCN budget as well as helping maintain stratospheric aerosol levels

35 (Williamson et al., 2019; Weigel et al., 2011; Brock et al., 1995). The properties of aerosols formed exhibit a seasonal variability, driven primarily by monthly differences in deposition (i.e., rainfall) and gas emissions (Alves et al., 2016). Despite this significance, the chemistry and dynamics of particle formation and growth over the Amazon is not completely understood. NPF is rarely observed near the ground (Martin et al., 2010), in contrast to remote forested locations in other regions of the world where NPF is observed more frequently (e.g., Andreae et al., 2022; Dada et al., 2018; Dal Maso et al., 2008). Nevertheless,

40 periodic "bursts" of UAPs where little to no growth is apparent have been observed at ground level. For example, a multi-year statistical analysis of size distribution data collected at the Cuieiras forest reservation in central Amazonia revealed that nearly one-third of the observation days featured undefined bursts of UAPs that did not appear to grow from local ground-level NPF events (Rizzo et al., 2018). Although formation is rarely seen near the surface, studies have observed intense NPF activity in the Amazon free troposphere (Andreae et al., 2018; Fan et al., 2018; Wang et al., 2016), where it is thought gaseous precursors are

45 brought by convective updrafts and nucleation occurs due to low temperature and particle surface area conditions (Zhao et al., 2020; Williamson et al., 2019; Weigel et al., 2011). Freshly nucleated particles, in turn, can be brought to the boundary layer by convective downdrafts and grow to larger sizes by coagulation and condensation of BVOC oxidation products (Andreae et al., 2018; Wang et al., 2016; Merikanto et al., 2009; Ekman et al., 2008). A recent study demonstrated that nucleation of organic vapors could serve as the primary formation pathway for these particles (Zhao et al., 2020), but the molecular identities

50 of the species involved and their seasonal variability remain largely unknown. Direct observations of UAP composition could help elucidate these formation and growth pathways and bridge the gap between what is known of the gas emissions and the composition of larger aerosol particles.

Secondary products of BVOCs seem to contribute substantially to aerosol particle mass in the Amazon basin (Martin et al., 2010). Near the surface, it is thought UAP formation is primarily driven by nucleation of sulfuric acid due its extremely low

55   volatility, after which new particle growth can occur by reactive uptake and condensation of other low volatility species such as oxygenated organic molecules (Ehn et al., 2014; Sipilä et al., 2010). Isoprene, the dominant VOC emitted by regional vegetation (Guenther et al., 2012), has been estimated to contribute substantially to aerosol particle mass principally via the condensation of products formed from reactions with OH radical (Isaacman-VanWertz et al., 2016; Chen et al., 2015). One such product, an organosulfate formed from the heterogeneous uptake of isoprene epoxydiol (IEPOX) onto sulfuric acid seed particles, has been

60   observed in central Amazonia across different seasons, accounting for up to nearly 90% of organic sulfate observed in low-NOx conditions (Glasius et al., 2018). Secondary products of monoterpenes have also been observed in Amazon particles, such as 3-methyl-1,2,3-butanetricarboxylic acid (MBTCA) and pinic acid (Leppla et al., 2023; Kourtchev et al., 2016; Kubátová et al., 2000). Due to the lack of particle size resolution in these measurements, particularly in the ultrafine range, it is difficult to comment on the extent to which these species are relevant to particle formation or growth in the region. Glicker et al. (2019)

65   indirectly observed IEPOX in UAPs in central Amazonia during the Observations and Modeling of the Green Ocean Amazon (GoAmazon2014/5) experiment using a thermal desorption chemical ionization mass spectrometer. The dominant positive ion observed throughout the measurement period was tentatively identified as an IEPOX thermal decomposition product (3-methylfuran, m/z 83) (Allan et al., 2014), implicating the role isoprene oxidation has on new particle growth in the region. Glicker et al. (2019) also observed significant changes in UAP composition between background or "pristine" periods and

70   periods of anthropogenic emission influence from the city of Manaus (located 70 km west from site). Distinct compositional differences between anthropogenic and background periods were also observed in larger particles (PM1) using an aerosol mass spectrometer at the same site during a different time of the year (de Sá et al., 2019), speaking to the sensitivity of particle growth pathways to human activity in the Amazon. Besides urban emissions, biomass burning has been shown to have to have a significant impact on particle composition, particularly in months with less rainfall (e.g., de Sá et al., 2019; Kourtchev et al.,

75   2016). Encroaching influence from deforestation, wildfires, and drought are projected to increase in the coming decades (Flores et al., 2024), causing disturbances in the Amazon ecosystem and potentially intensifying regional climate change. Evidence already exists that the distribution of BVOCs in the Amazon are in a state of transition in response to human activity (Yáñez-Serrano et al., 2020). Gaining molecular insight into the species responsible for regional particle formation is critical to efforts that will seek to model how these processes could change and thus impact global climate systems in the future.

80   Here, we present tree-canopy level observations of UAP molecular composition at a site located within the Tapajós National Forest of eastern Amazonia. To gain insight into the seasonal differences in the sources contributing to particle formation and growth in the region, UAPs were collected during the months September and December of 2016 (dry season) and June of 2017 (late wet season). With an annual rainfall of 1920 mm (Saleska et al., 2003), the Tapajós forest is comparatively drier than other extensive Brazilian wet forests, and has therefore been thought of as a predictive model forest for the larger Amazon ecosystem

85   in future climate change scenarios (Cox et al., 2000).

3 Methods

3.1 Site description

Measurements were performed at the Santarém-Km67-Primary Forest (BR-Sa1) tower site in the Tapajós National Forest (2.857° S, 54.959° W), located near kilometer 67 of the Santarém-Cuiabá highway and about 50 km south of Santarém, Pára, Brazil. This site is part of the AmeriFlux and Large-scale Biosphere-Atmosphere Experiment in Amazonia (LBA) networks. Tapajós National Forest is comprised primarily of old-growth evergreen species (Saleska, 2019) and experiences a wet season extending from January to June, and a dry season from mid-July through December (da Rocha et al., 2009; Saleska et al., 2003).

3.2 Ultrafine particle collection

Aerosol particles were sampled near the top of the tree canopy by connecting ground-level instruments to a 30 m long inlet (Fig. S1 in the Supplement). UAPs (5 - 70 nm in mobility diameter) were impacted onto pre-baked aluminum foil substrates using a sequential spot sampler (Aerosol Devices Inc.) (Fernandez et al., 2014) after being size-selected with a nano differential mobility analyzer (nano-DMA; TSI, model 3085). Foil substrates were placed inside wells of a 33-well rotating sample disk, which collected for a period of 22 h per well followed by a 2 h blank collection in a separate well. The blank consisted of particle-free air sampled by setting the voltage of the nano-DMA to zero, which efficiently removes all particles from the sample stream. Number-size distributions of the collected particles were measured in parallel by counting selected UAPs using a mixing condensation particle counter (Brechtel Manufacturing Inc., model 1720). Periodic size distribution measurements spanning from September 2016 - June 2017 at the Km67 site are shown in Fig. S2. UAPs were collected for compositional analysis during three different seasonal periods: 10 - 30 September 2016 (sample hereafter referred to as SEP), 18 November - 23 December 2016 (DEC), and 22 May - 21 June 2017 (JUN). After collection, sample plates were wrapped in clean aluminum foil, sealed with Teflon tape, and stored at -4 °C until analysis.

3.3 LC/MS analysis

Sample foils from each measurement period were pooled together into a vial (1 month/vial) for extraction in 600 μL of acetonitrile (Sigma-Aldrich, HPLC grade) for 5 h at room temperature (21 °C). Blank collection foils were pooled and extracted in the same manner to serve as background signal. Extracts were then transferred into clean vials and evaporated under a gentle stream of nitrogen to a final volume of 50 μL.

An LC/MS methodology was adopted in the present study to ensure the acquisition of usable spectra with very low sample volume available as well as to reduce artifact-inducing effects of ion suppression that has been observed in the analysis of complex organic aerosols with direct infusion (Kourtchev et al., 2020). Samples were analyzed with an ultrahigh performance liquid chromatograph (Vanquish UHPLC, Thermo Fisher) coupled to an Orbitrap mass spectrometer (Q Exactive Plus, Thermo Fisher), which has a mass resolving power of $\sim 10^5$ at m/z 200 and is equipped with a heated electrospray ionization inlet

(HESI). A Luna 1.6 μm Omega Polar C18 (150 × 2.1 mm) (Phenomenex) heated at 30 °C was used as the stationary phase, while an eluent system consisting of (A) 0.1% (v/v) formic acid in water (HPLC grade, Sigma Aldrich) and (B) 0.1% formic acid in acetonitrile (HPLC grade, Sigma Aldrich) was used as the mobile phase. A sample volume of 10 μL was injected at a

120 flow rate of 300 μL/min and subjected to the following 22 min gradient elution: 3.0 min hold at 95% eluent A, 11 min ramp to 95% eluent B, 2.0 min hold at 95% eluent B, 6.0 min hold at 95% eluent A. The HESI inlet was set to a potential of 2.5 kV and a capillary temperature of 320 °C, with inlet flows of 50, 10, and 1 for sheath, auxiliary (heated to 300 °C), and sweep gases, respectively. Ions were scanned in the negative ion mode from 100 - 1500 amu, while the top 3 most abundant ions from each scan were selected for MS/MS analysis by higher-energy collisional dissociation (Olsen et al., 2007). Xcalibur software

125 (version 3.1, Thermo Fisher) was used for data acquisition.

LC/MS data was processed following a methodology developed by Nizkorodov et al. (2011) that has been used in the analysis of organic aerosol samples previously (e.g., Baboomian et al., 2022; Maclean et al., 2021). Briefly, Freestyle software (version 1.6, Thermo Fisher) was used to view and integrate ion chromatograms in the region where analyte signal was observed (1 - 10 min). Decon2LS software (Jaitly et al., 2009) was then used to extract peak positions and intensities. Home-built LabVIEW

130 programs (National Instruments Corp.) were used to remove peaks containing ^{13}C and ^{34}S isotopes and assign background-subtracted analyte peaks with the following formula constraints: $C_{1-40}H_{2-80}O_{1-35}N_{0-3}S_{0-2}$, H/C ratios of 0.2 - 2.25, O/C ratios of 0 - 4, double bond equivalents (DBE) of -0.5 - 16.5. Only peaks with m/z 100 - 700 were considered for assignment due to low analyte abundance above this range.

3.4 Volatility prediction

135 Compound volatility distributions were predicted using the assigned molecular formulae from the HRMS data following Li et al. (2016). Volatilities are reported as the saturation concentrations of the pure organic vapors (C_0) predicted using the parameterization:

$$\log_{10} C_0 = (n_C^0 - n_C)b_C - n_O b_O - 2\frac{n_C n_O}{n_C + n_O}b_{CO} - n_N b_N - n_S b_S \tag{1}$$

where n_C, n_O, n_N, and n_S refers to the number of carbon, oxygen, nitrogen, and sulfur atoms, respectively. Values used for

140 the parametric coefficients n_C^0, b_C, b_O, b_N, and b_S were determined following those provided for the CHO, CHON, and CHOS compound classes in Li et al. (2016).

3.5 Meteorology and complementary datasets

Six-hour back-trajectory frequency simulations were calculated over the three seasonal periods discussed in this study using the NOAA Hybrid Single-Particle Lagrangian Integrated Trajectory (HYSPLIT) transport model (https://www.ready.noaa.

145 gov/HYSPLIT.php, last accessed March, 2024) with GDAS 1° meteorology (Rolph et al., 2017; Stein et al., 2015). Fire occurrence data was visualized using the Fire Information for Resource Management System (FIRMS) from NASA (https://www.earthdata.nasa.gov/learn/find-data/near-real-time/firms, last accessed May, 2024), which compiles thermal anomaly data obtained from the Moderate Resolution Imaging Spectroradiometers (MODIS) aboard the Terra and Aqua satellites (data dis-

claimer link: https://www.earthdata.nasa.gov/learn/find-data/near-real-time/citation#ed-lance-disclaimer) (Giglio et al., 2018).

150   Meterological ERA5 reanalysis data from the European Centre for Medium-Range Weather Forecasts (Hersbach et al., 2023) was obtained from their Climate Data Store (https://cds.climate.copernicus.eu, last accessed June 2024) to receive parameters of surface temperature, dew point temperature, precipitation, solar radiation at surface, cloud cover, total atmospheric column water, boundary layer and cloud base height, and leaf area index at the measurement site (2.9° S, -55° W) with 0.25° resolution during each collection period.

155   **4   Results and discussion**

Fig. 1 shows the average mass spectra obtained for the JUN, SEP, and DEC samples. Only assigned species are shown, corresponding to 77%, 92%, and 76% of the total ion intensity attributed to the the JUN, SEP, and DEC samples, respectively. Ion peaks are colored based on their assigned molecular formulae, categorized into four compound classes: CHO (black), CHON (blue), CHOS (red), and CHONS (green). Also included are the ion intensity-based distributions of each compound

160   class in the different months. Percent values shown correspond to the fraction of total assigned ion intensity attributed to the sum of species from each of the four compound classes. The CHO class (species only containing carbon, hydrogen, and oxygen atoms) composed the majority of assigned intensity for all three months (52 - 59%). The CHOS class was the second most abundant category in JUN and SEP, while the CHON class was more dominant in DEC. CHONS compounds composed the smallest class observed, accounting for only 2 - 6% of assigned ion intensity. The single most abundant ion identified in both

165   JUN and SEP was m/z 215.023, corresponding to a compound with the electrically neutral molecular formula $C_5H_{12}O_7S$. The molecule is tentatively identified as an IEPOX-derived organosulfate species (IEPOX-OS) based on its formula as well as the prominent loss of bisulfate (HSO_4^-) in its MS2 fragmentation spectrum (Fig. S3), a distinguishing feature of organosulfate species (Attygalle et al., 2001). As noted above, IEPOX-OS species have been observed previously in Amazon aerosol particles (Glasius et al., 2018; Kourtchev et al., 2016), and their persistent presence in ultrafine particles observed here irrespective of

170   season implicates isoprene organosulfate chemistry as a key player in new particle growth in the Amazon year-round. Despite this consistency, the UAPs sampled also exhibited substantial compositional variation, offering evidence for seasonal variability in emission sources and formation pathways.

4.1   Seasonality of marker ion distributions

A summary of different species that are representative of key sources and processes, herein referred to as "marker ions,"

175   have been identified in each month and are shown in Fig. 2A. The species listed represent four different potential sources based on their assigned molecular formula: primary biogenic organic aerosol (PBOA), monoterpene-derived secondary organic aerosol (MT SOA), isoprene-derived secondary organic aerosol (isopene SOA), and biomass burning organic aerosol (BBOA). Together, the marker species included account for 55%, 40%, and 16% of the total assigned ion intensity (or 42%, 37%, and 12% when including unassigned intensity) for JUN, SEP, and DEC, respectively. Table S1 shows a full list of markers

180   identified with suggested chemical structures and references. It should be noted that since ion percents are calculated as an
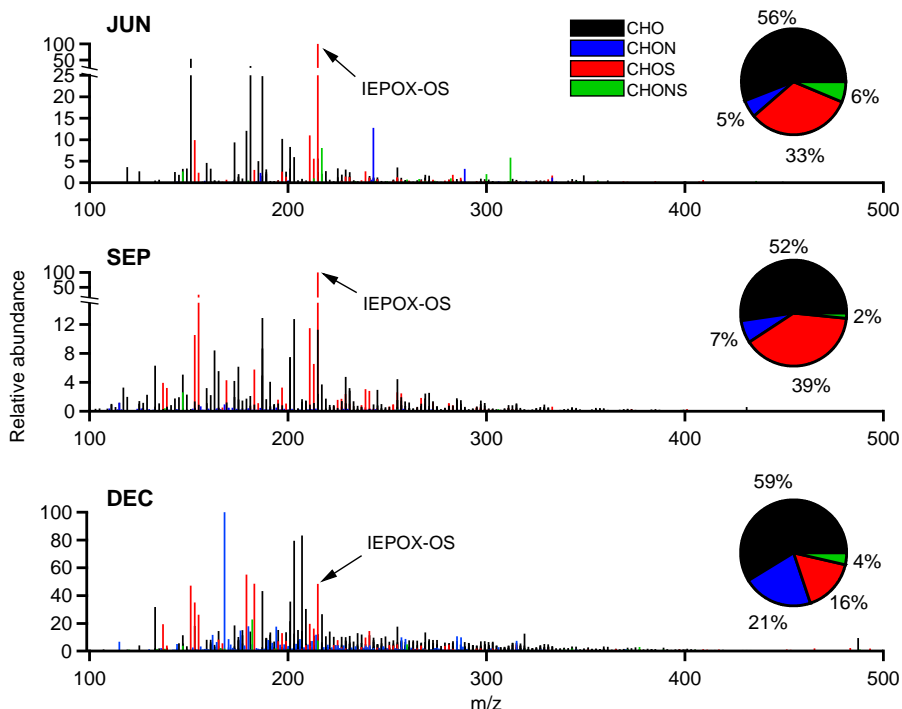
Figure 1. Average mass spectra of assigned species in the three months sampled. Color of individual peaks indicates assigned compound class: CHO (black), CHON (blue), CHOS (red), or CHONS (green). On the right side of each spectrum is overlaid a pie chart displaying the summed ion abundance of each compound class as a fraction of total assigned intensity.

average over analyte retention time, and since most identifications are based solely on the molecular formulae assigned, the ion signal attributed to species with these formulae may include several isomers. Although CHO compounds comprised the largest fraction of ion intensity in all three months sampled, the most abundant species contributing to this compound class varied with season. During the late wet season (JUN), the top two most abundant CHO compounds were *m/z* 151.0612 (with

185   an electrically neutral formula $C_5H_{12}O_5$) and *m/z* 181.0718 ($C_6H_{14}O_6$), tentatively identified as the sugar alcohols arabitol and mannitol, respectively. These two species have previously been used as markers for PBOA (Samaké et al., 2019; Nirmalkar et al., 2015; Bauer et al., 2008), being found in fungal spores where they are used as energy storage products (Lewis and Smith, 1967). Lawler et al. (2020) previously observed these species in UAPs in the southeastern U.S. using thermal desorption chemical ionization mass spectrometry, finding that the concentration of UAPs containing these species spiked during periods

190   of heightened rainfall. That study concluded that the observed UAPs formed from fungal spores, which fragmented upon exposure to rainfall and/or high humidity. Biological spore samples collected from the Amazon have previously been observed to fragment under high humidity, such as those during the wet season, resulting in the formation of UAPs (China et al., 2016). High concentrations of airborne fungal spores have also been linked to rainfall events (Huffman et al., 2013), and particles enriched in biogenic salts linked to fungal spores have been observed in the Amazon wet season (Pöhlker et al., 2012; Lawson

195 and Winchester, 1979). To the best of our knowledge, our observations here represent the first chemical evidence for the occurrence of airborne ultrafine fungal fragments in the Amazon rainforest, as a previously unaccounted source of UAPs in the region. The fact that these ions were more abundant in JUN suggest that this process may be particularly important during the wet season, but more measurements are needed to confirm spatiotemporal prevalence. In addition to arabitol and mannitol, another abundant CHO species in JUN was glucose ($C_6H_{12}O_6$, *m/z* 179.0561), a known marker from plant material such as
200 pollen fragments (Samaké et al., 2019).

The most abundant CHO species in SEP likely were derived from monoterpene oxidation. To help corroborate this, the ion chromatograms and tandem mass spectra obtained for some of these species were compared to those of species observed in α-pinene ozonolysis particles. Bulk ozonolysis particles were collected in a set of laboratory experiments using the spot sampler operating at similar conditions to those used in the present study. Details for these experiments are provided in the
205 Supporting Information. The most abundant species observed was $C_8H_{12}O_5$ (*m/z* 187.061) and is identified as an isomer(s) of hydroxyterpenylic acid, a proposed marker for α-pinene oxidation (Kahnt et al., 2014). Similar fragments are observed when comparing the MS2 for this ion to literature, including the dominant product ion at *m/z* 125.024 (ion formula $C_6H_5O_3^-$) (Fig S4). This species was also the most abundant monoterpene oxidation marker identified in JUN and DEC, suggesting that this compound may serve as a suitable marker at different times of the year in the Amazon. An unknown species (excluded
210 from Fig. 2A) with the same unit mass (*m/z* 187.098, $C_9H_{16}O_4$) found in SEP and DEC has a similar retention time to an α-pinene ozonolysis product observed in our experiments (Fig. S5), although it is likely that several isomers are present with different retention times. The second most abundant CHO species in SEP had a molecular formula $C_8H_{12}O_6$ and is identified as 3-methyl-1,2,3-butanetricarboxylic acid (MBTCA), a marker for the multigeneration oxidation of monoterpenes (Szmigielski et al., 2007). Other studies have found MBTCA in particles from the central Amazon, both observing higher signals in the
215 dry season (Glasius et al., 2018; Kourtchev et al., 2016) compared to the wet season. This is consistent with the idea that photochemical processing may be more prominent during the dry season when there is likely to be more solar radiation penetrating to the surface, reaching a maximum around August/September in the nearby city of Santarém (Reis et al., 2022). Corroborating this, ERA5 reanalysis data from the measurement site also shows highest average daytime solar radiation at the surface during SEP (Table S2). It is also worth noting that monoterpene emissions have been observed to peak during the
220 Amazon dry season (Alves et al., 2022; Yáñez-Serrano et al., 2018), helping explain the overall abundance of these markers during SEP. Comparison of the MS2 spectrum for this ion with that of a product with a similar retention time from the α-pinene ozonolysis experiments suggests structural similarities, including evidence for more than one carboxylic acid group (Figs. S6 and S7). It is intriguing that the lower molecular weight MT SOA markers in general show highest abundance in JUN whereas the heavier species starting with $C_8H_{12}O_6$ show highest abundance in SEP, possibly suggesting a seasonal dependence of
225 reaction branching ratios. Another possible driver of these differences is a seasonal dependence of monoterpene speciation. For instance, Yáñez-Serrano et al. (2018) observed stark seasonal differences in monoterpene distributions in Central Amazonia, observing higher relative abundance of α-pinene and limonene in the dry season (August, October) and α-terpinene and 3-carene in the late wet season (June). The species $C_5H_8O_5$, identified as 3-hydroxyglutaric acid (Claeys et al., 2007), has also been observed as an oxidation product of isoprene from a non-IEPOX pathway (Liu et al., 2016a; Krechmer et al., 2015),
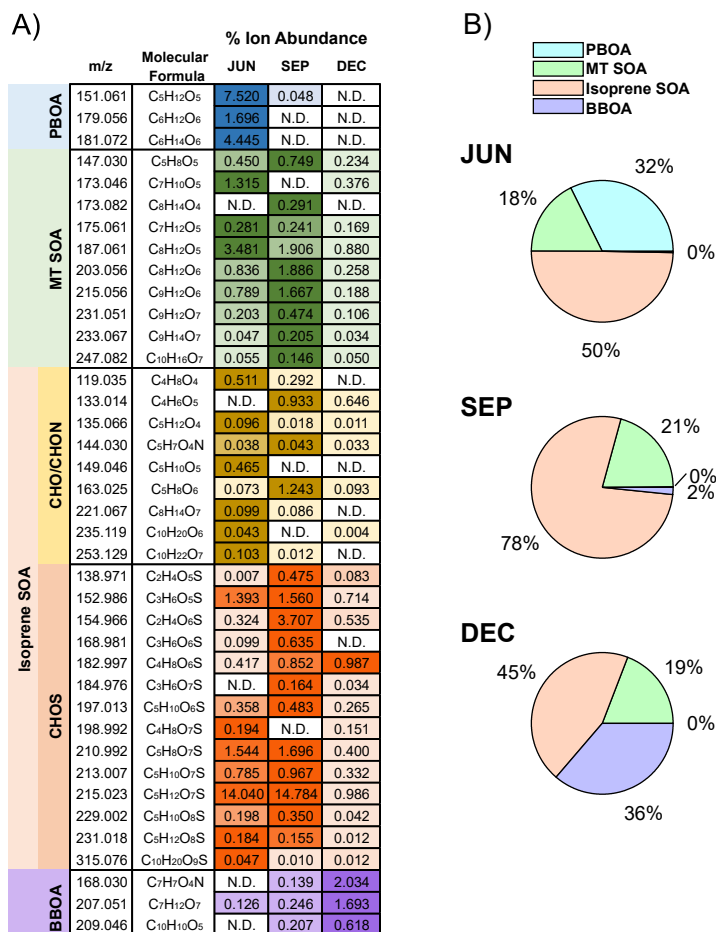
A)

	m/z	Molecular Formula	% Ion Abundance		
			JUN	SEP	DEC
PBOA	151.061	$C_5H_{12}O_5$	7.520	0.048	N.D.
	179.056	$C_6H_{12}O_6$	1.696	N.D.	N.D.
	181.072	$C_6H_{14}O_6$	4.445	N.D.	N.D.
MT SOA	147.030	$C_5H_8O_5$	0.450	0.749	0.234
	173.046	$C_7H_{10}O_5$	1.315	N.D.	0.376
	173.082	$C_8H_{14}O_4$	N.D.	0.291	N.D.
	175.061	$C_7H_{12}O_5$	0.281	0.241	0.169
	187.061	$C_8H_{12}O_5$	3.481	1.906	0.880
	203.056	$C_8H_{12}O_6$	0.836	1.886	0.258
	215.056	$C_9H_{12}O_6$	0.789	1.667	0.188
	231.051	$C_9H_{12}O_7$	0.203	0.474	0.106
	233.067	$C_9H_{14}O_7$	0.047	0.205	0.034
	247.082	$C_{10}H_{16}O_7$	0.055	0.146	0.050
CHO/CHON	119.035	$C_4H_8O_4$	0.511	0.292	N.D.
	133.014	$C_4H_6O_5$	N.D.	0.933	0.646
	135.066	$C_5H_{12}O_4$	0.096	0.018	0.011
	144.030	$C_5H_7O_4N$	0.038	0.043	0.033
	149.046	$C_5H_{10}O_5$	0.465	N.D.	N.D.
	163.025	$C_5H_8O_6$	0.073	1.243	0.093
	221.067	$C_8H_{14}O_7$	0.099	0.086	N.D.
	235.119	$C_{10}H_{20}O_6$	0.043	N.D.	0.004
	253.129	$C_{10}H_{22}O_7$	0.103	0.012	N.D.
CHOS	138.971	$C_2H_4O_5S$	0.007	0.475	0.083
	152.986	$C_3H_6O_5S$	1.393	1.560	0.714
	154.966	$C_2H_4O_6S$	0.324	3.707	0.535
	168.981	$C_3H_6O_6S$	0.099	0.635	N.D.
	182.997	$C_4H_6O_6S$	0.417	0.852	0.987
	184.976	$C_3H_6O_7S$	N.D.	0.164	0.034
	197.013	$C_5H_{10}O_6S$	0.358	0.483	0.265
	198.992	$C_4H_8O_7S$	0.194	N.D.	0.151
	210.992	$C_5H_8O_7S$	1.544	1.696	0.400
	213.007	$C_5H_{10}O_7S$	0.785	0.967	0.332
	215.023	$C_5H_{12}O_7S$	14.040	14.784	0.986
	229.002	$C_5H_{10}O_8S$	0.198	0.350	0.042
	231.018	$C_5H_{12}O_8S$	0.184	0.155	0.012
	315.076	$C_{10}H_{20}O_9S$	0.047	0.010	0.012
BBOA	168.030	$C_7H_7O_4N$	N.D.	0.139	2.034
	207.051	$C_7H_{12}O_7$	0.126	0.246	1.693
	209.046	$C_{10}H_{10}O_5$	N.D.	0.207	0.618

B)

PBOA
MT SOA
Isoprene SOA
BBOA

JUN
32%
18%
0%
50%

SEP
21%
0%
2%
78%

DEC
45%
19%
0%
36%

Figure 2. Distribution of emission marker species observed in each month. (A) Heatmap of individual ion abundances normalized by total ion abundance (assigned and unassigned) in units of percent. Colors correspond to the different emission source classes: primary biogenic organic aerosol (PBOA, in blue), monoterpene-derived secondary organic aerosol (MTSOA, in green), isoprene-derived secondary organic aerosol (Isoprene SOA, yellow and orange), and biomass burning organic aerosol (BBOA, in purple). For each ion, darker shades correspond to greater normalized abundance for that species relative to other months. (B) Pie chart showing the contribution of each emission source class as a percent of total marker ion intensity.

230 although it is used as a monoterpene marker here since the IEPOX pathway is likely to dominate during the Amazon wet season (Shrivastava et al., 2019). Relative to JUN and SEP, DEC had a lower contribution of secondary markers from both monoterpenes and isoprene. It should be noted that other compounds of anthropogenic origin such as aromatic hydrocarbons could be driving unaccounted secondary formation as well. Oxidation flow reactor measurements of ambient gases conducted

in the Central Amazon previously found that a large fraction of observed SOA formation during the dry season could not be
235 reconciled using known formation potentials of terpenoids alone (Hodshire et al., 2018; Palm et al., 2018).

In all three months, isoprene SOA accounted for the largest fraction of the identified marker ion intensity (Fig. 2B). Isoprene
organosulfates were the most dominant isoprene-derived compounds observed for each month, and contributed the most ion
abundance to SEP (28% of assigned intensity). Isoprene emissions and the formation of gas phase oxidation products such as
IEPOX typically peak in the Amazon dry season due to higher solar intensity and ambient temperatures relative to the wet
240 season (Langford et al., 2022; Rinne et al., 2002), conditions reflected here in a comparison between JUN and SEP (Table
S2). Sarkar et al. (2020) observed a strong correlation between isoprene and monoterpene fluxes with temperature and solar
radiation at the same measurement site studied here in the Tapajós National Forest. Riva et al. (2019) found that increasing
the concentration ratio of IEPOX to inorganic sulfate drives the formation of organosulfate species. The dominance of these
species observed in SEP suggests that this ratio could be a key driver of organosulfate chemistry in the eastern Amazon, and
245 parallels observations of PM_1 composition in the Central Amazon where organic sulfate concentrations peaked in the dry
months (Glasius et al., 2018). Seasonal measurements of inorganic sulfate concentrations in UAPs would be needed to probe
the influence of this chemistry further, however. Compared to the other months, SEP also had the lowest average relative
humidity (Table S2). Several studies have correlated organosulfate formation with aerosol acidity, and have observed increased
uptake of isoprene products such as IEPOX onto acidic particles (Zhang et al., 2018; Liao et al., 2015; Surratt et al., 2007b).
250 Another possible explanation for the dominance of organosulates in SEP could therefore be that there was less water vapor
available to dilute the sulfate aerosols needed to form these species, allowing for more efficient reactive uptake to occur.

While still comprising the largest source fraction, the relative contribution of isoprene organosulfates to sample intensity was
nevertheless smallest in DEC, most notably IEPOX-OS. Corresponding to the end of the dry season and onset of the wet season,
one possible explanation for this is meteorology, given that DEC had the highest average cloud cover (82%) and total column
255 water (52 kg/m^2) of the three months studied (Table S2), possibly leading to lower IEPOX formation and uptake for the reasons
discussed above. Another possible factor is higher regional levels of NOx due to wildfire activity, leading to the suppression
of the IEPOX pathway by NO (Paulot et al., 2009). Although isoprene is generally expected to eventually form IEPOX via
the HO_2 oxidant pathway under pristine conditions, Liu et al. (2016b) showed evidence that under polluted conditions where
[NOy] > 1 ppb, isoprene photooxidation chemistry drastically shifts towards the NO pathway, producing oxidation products
260 such as methyl vinyl ketone instead of the HO_2-produced hydroxyhydroperoxides (ISOPOOH). At the same measurement
site in the Central Amazon (located 70 km west of the urban center Manaus), Liu et al. (2018) found that OH concentrations,
inferred from measured concentrations of isoprene photooxidation products, increased ~250% under similar polluted conditions,
indicating that the anthropogenic contribution of NOx has the potential to greatly impact oxidation pathways. Fig. 3(A) shows
air mass history analysis using HYSPLIT and panel (B) shows the distribution of fires observed via satellite from the MODIS
265 instrument over the course of the three seasonal periods. Although each period was dominated by easterly winds, the number
of fires observed varied substantially, with the most anomalies occurring in DEC. Corroborating satellite data is the abundance
of identified BBOA species in DEC including $C_7H_7O_4N$, $C_7H_{12}O_7$, and $C_{10}H_{10}O_5$, assigned to methyl-nitrocatechol, methyl
galacturonate, and a vanillin oxidation marker, respectively (Mabato et al., 2022; Kong et al., 2021; Iinuma et al., 2010). Under

the influence of NOx, isoprene reacts with OH radical and NO/NO$_2$ to form methacryloylperoxynitrate, which then can be

270 oxidized to form the aerosol markers 2-methylgylceric acid and 2-methylgylceric acid organosulfate (2-MG OS) (Nguyen et al., 2015; Surratt et al., 2007b). Compared to IEPOX-OS, 2-MG OS ($C_4H_8O_7S$, *m/z* 198.992) was observed to be a comparatively minor species, but it is notable that the ratio of 2-MG OS to IEPOX-OS was an order of magnitude greater in DEC compared to JUN (Fig. 2A), the month experiencing the least influence from regional wildfire activity (Fig. 3B). The only organosulfate species to have a greater relative contribution to ion intensity in DEC compared to the other months was $C_4H_8O_6S$, *m/z* 182.997.

275 Shalamzari et al. (2013) observed this compound in ambient filters from Hungary and through structural characterization via MS^n analysis hypothesized that the species was formed from the oxidation of methyl vinyl ketone, a first generation isoprene product formed via ozonolysis or by OH oxidation in the presence of NOx (Liu et al., 2013; Barket et al., 2004; Aschmann and Atkinson, 1994). Besides isoprene oxidation, methyl vinyl ketone can also be emitted from biomass burning of tropical forest fuels (Karl et al., 2007) . Additionally, two nitrooxy isoprene OS species (Surratt et al., 2008) were identified

280 in the dry season months (SEP, DEC) (Table S1): $C_5H_{11}O_9NS$ and $C_5H_9O_{12}N_2S$. The identification of these species further supports the hypothesis that isoprene chemistry may have been influenced by NOx enrichment in the dry season. In all, these observations suggest anthropogenic emission sources such as biomass burning could be impacting isoprene organosulfate formation processes in Amazonian UAPs, impacts liable to increase in coming decades with further human activity in the region.

285 Organic sulfur compounds from sources besides isoprene were also identified in all three samples, but most prominently represented in SEP and DEC (Table S1). For instance, the most abundant CHOS species in DEC was $C_6H_{12}O_4S$, *m/z* 179.0385, and is attributed to the SO$_2$-initiated photooxidation of polycyclic aromatic hydrocarbons (Jiang et al., 2022), such as those emitted during biomass burning (Jenkins et al., 1996). Other abundant CHOS species in DEC possibly derived from similar sources include $C_4H_8O_4S$ and $C_2H_4O_6S$ (Jiang et al., 2021; Kuang et al., 2016). Monoterpene-derived organosulfate species

290 (MT-OS) were also identified, though in relatively low abundance, with the sum of MT-OS compounds in each month contributing <0.7% of total ion signal. Interestingly, the highest number of MT-OS compounds (8) were identified in DEC, including $C_7H_{12}O_7S$, $C_9H_{16}O_6S$, and $C_7H_{12}O_6S$. In addition, two nitrooxy MT-OS species were identified and solely present in DEC: $C_{10}H_{17}O_7NS$ and $C_9H_{15}O_8NS$. These species have previously been proposed to form from either nitrate radical oxidation or photooxidation in the presence of NOx, both in the presence of acidic sulfate particles (Surratt et al., 2008).

295 Species with molecular formulae of non-organosulfate isoprene markers were also identified in each month (Fig. 2A), including 2-methyltetrol ($C_4H_8O_4$, *m/z* 119.0350) and 2-methyltartaric acid ($C_5H_8O_6$, *m/z* 163.0250) (Jaoui et al., 2019; Claeys et al., 2004). Interestingly, most of the CHO isoprene markers identified were most abundant in JUN. Given that this month experienced the highest average relative humidity, a possible explanation would be that these products were formed under less acidic conditions in particles, hindering the subsequent oxidation by sulfuric acid to form their organosulfate counterparts.

300 Regarding possible humidity effects, it is also worth noting that 2-methyltetrol, formed from the particle-phase hydrolysis of IEPOX, and its dimer ($C_{10}H_{22}O_7$, *m/z* 253.1293) are most abundant in JUN (Armstrong et al., 2022; Riva et al., 2019; Surratt et al., 2007a). Conversely, the IEPOX-OS dehydration product $C_5H_{10}O_6S$ (*m/z* 197.0125) is most abundant SEP, the driest month observed. Finally, a marker for the oxidation of isoprene by nitrate radical was also identified ($C_5H_7O_4N$, *m/z* 144.0302)
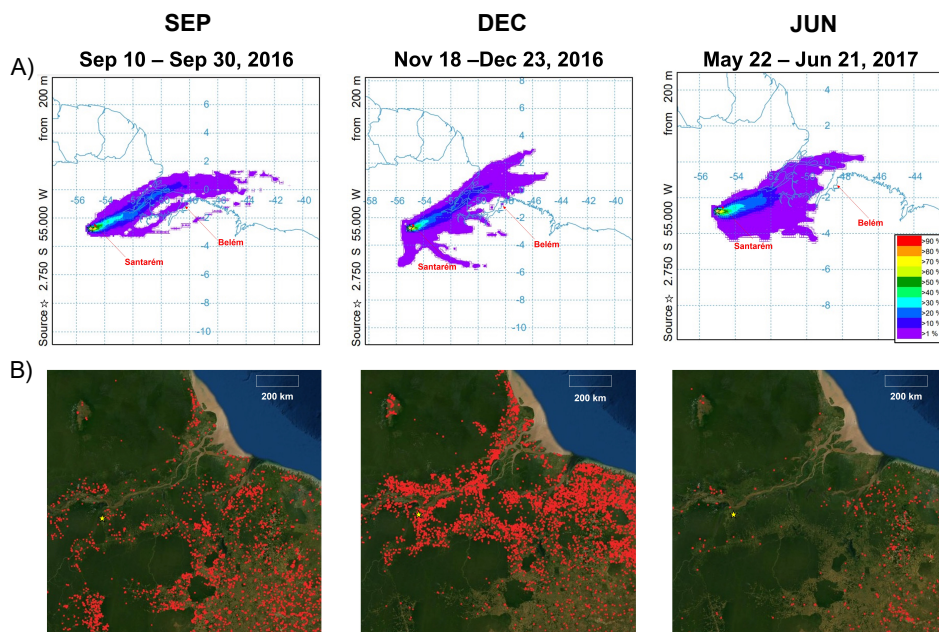
Figure 3. (A) Air mass back-trajectory frequencies from HYSPLIT for each seasonal period studied. 48 h back-trajectories were integrated over the time span of each period at a height of 200 m above ground level (near tree canopy). The color scale indicates how frequently air masses passed over a given location, with warmer color indicating higher frequencies. (B) MODIS fire observations from the Aqua and Terra satellites as visualized using FIRMS integrated over each period. Each red dot indicates a thermal anomaly identified as a probable fire occurrence. The yellow star indicates the location of the measurement site in each plot.

(Rollins et al., 2009). The ion fraction of this species was rather consistent across all three months, suggesting that this process
305 may serve as a regular (likely nighttime due to reaction with nitrate) source of UAP growth in the region irrespective of season.

4.2 Seasonality of aerosol molecular properties

In addition to differences in the marker ions, differences in the molecular properties of all species observed in each month such as the distribution of oxidation states and degree of unsaturation were also investigated. Fig. 4 depicts the carbon oxidation states and double bond equivalents of the CHO-containing molecules observed in each period. Carbon oxidation state (OS_C)
310 was estimated following Kroll et al. (2011):

$$OS_C \approx 2O/C - H/C \qquad (2)$$

where O/C and H/C refer to the ratio of oxygen to carbon atoms and hydrogen to carbon atoms, respectively. It should be noted that the presence of some functionalities such as peroxides will lead to an overestimation of carbon oxidation state. Nevertheless, this estimate serves as a relative means to compare the extent of oxidation of molecules in each period. Most species
315 observed had OS_C values between -1 and 1, corresponding to the oxidation range associated with semi- and low volatility oxidized organic aerosol components (Kroll et al., 2011). Compared to JUN, higher oxidation states were observed in SEP and
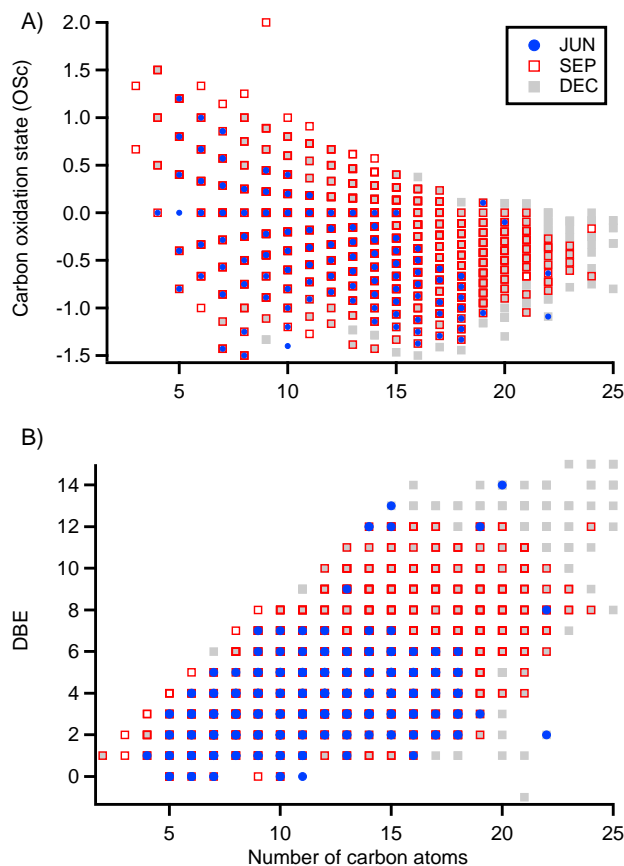
Figure 4. Comparison of (A) carbon oxidation state and (B) double bond equivalents of CHO-containing molecules observed in each seasonal period.

DEC across most carbon numbers. Using measurements of reactive gases, previous studies have shown that OH reactivity is highest during the Amazon dry season (Pfannerstill et al., 2021; Nölscher et al., 2016) coinciding with the seasonal peak in BVOC emissions and sunlight. These factors, coupled to the fact that potentially fewer products are lost due to wet deposition,

320   can thus be thought of as optimized for the multigeneration oxidation of organics during the dry season. Higher molecular weight CHO species were also observed in SEP and DEC. Baboomian et al. (2022) found that UV-aged SOA components were on average more oxidized, unsaturated, and heavier than those from fresh aerosol, attributing this to condensed-phase photochemical reactions. In line with this, CHO species observed in JUN were also more saturated compared to SEP and DEC (Fig. 2B). Besides the possible influence of photochemistry, biomass burning organics can also be highly unsaturated, with

325   oxygenated aromatic and nitroaromatic species as known markers (Bianchi et al., 2019; Iinuma et al., 2010).

Fig. 5 depicts the distribution of highly unsaturated CHON molecules (DBE $\geq$ 6) across the periods. CHON was the smallest compound class in JUN by ion abundance, and had the lowest number of observed molecular formulae (65 molecules assigned),
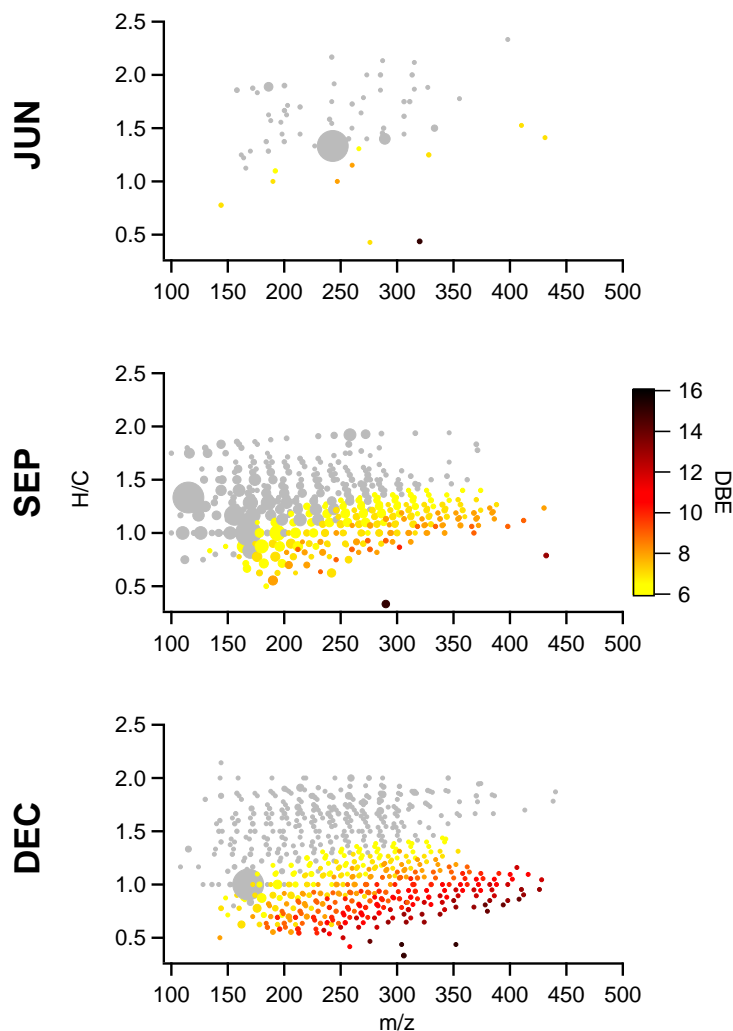
Figure 5. Distribution of double bond equivalents (DBE) for CHON-containing molecules observed in each seasonal period. Marker size indicates ion relative abundance.

most of which were relatively saturated. While more unsaturated species were observed in SEP, the most highly unsaturated CHON species were observed in DEC, possibly due to wildfire influence. Kourtchev et al. (2016) observed a similar trend in

330 bulk organic aerosol collected from Central Amazonia, also suggesting the influence from BBOA aromatics. Fig. S8 shows a similar trend apparent for CHO molecules. Fig. 6 depicts the distribution of CHON species in Van Krevelen space. In addition to being more saturated, CHON molecules observed in JUN were also less oxidized compared to the peak dry season (SEP), suggesting that aging processes such as photochemistry that could be affecting the CHO fraction are likely also influencing

nitrogen containing species in the dry months. A similar trend is observed when comparing JUN to DEC as well (Fig. S9),
335   though most of the most abundant ions appear to have similar O/C ratios.
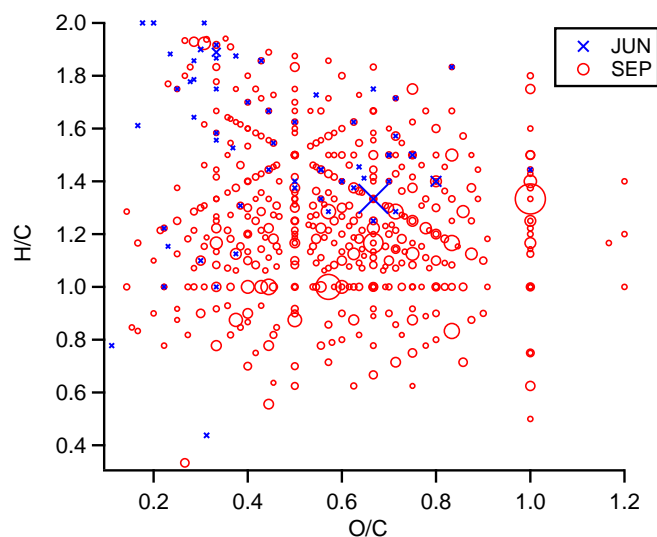
Figure 6. Van Krevelen diagram of the CHON molecules observed in JUN (blue circles) and SEP (red squares). Marker size indicates relative ion abundance.

Using a molecular corridor parameterization (Li et al., 2016), the volatilities of UAP constituents were estimated in each seasonal period for each compound class (Fig. 7). Most species observed in each period were either classified as semivolatile organic compounds (SVOC), defined as having saturation mass concentrations C_0 between 0.3 and 300 $\mu g/m^3$, or low volatility organic compounds (LVOC) ($3 \times 10^{-4} < C_0 < 0.3$ $\mu g/m^3$) (Murphy et al., 2014; Donahue et al., 2011). Although these species

340   are most likely not present at concentrations needed to initiate particle formation at the surface, it should be noted that many species classified as SVOC or LVOC at standard temperature and pressure (298 K, 1 atm) are classified as lower volatility species in the upper atmosphere, where temperatures are much lower. This is consistent with prior observations that Amazon UAPs are largely formed in the free troposphere (Zhao et al., 2020). Fig. S2 shows particle size distributions at the site from September 2016 through June 2017 (Fig. S2A), as well as the time-averaged distributions for the three seasonal periods (Fig.

345   S2B). No clear NPF events were observed at the surface during any of the periods, though highest UAP number concentrations were detected during the drier months (late June, September - December). Rizzo et al. (2018) observed a similar seasonal dependence of particle concentrations in central Amazonia, with the dry season being dominated by accumulation mode (~100 - 600 in diameter) particles, possibly contributed by regional biomass burning events. The average size distributions bear a striking resemblance across the different periods, suggesting that any differences in aerosol molecular properties including

350   volatility are not due to the sampled particle size.

Isoprene organosulfates including IEPOX-OS ($C_5H_{12}O_7S$, $C_0 = 0.16$ $\mu g/m^3$) dominate the LVOC fraction, particularly in JUN and SEP (Fig. 7). This is consistent with Lopez-Hilfiker et al. (2016), who classified IEPOX SOA components as low
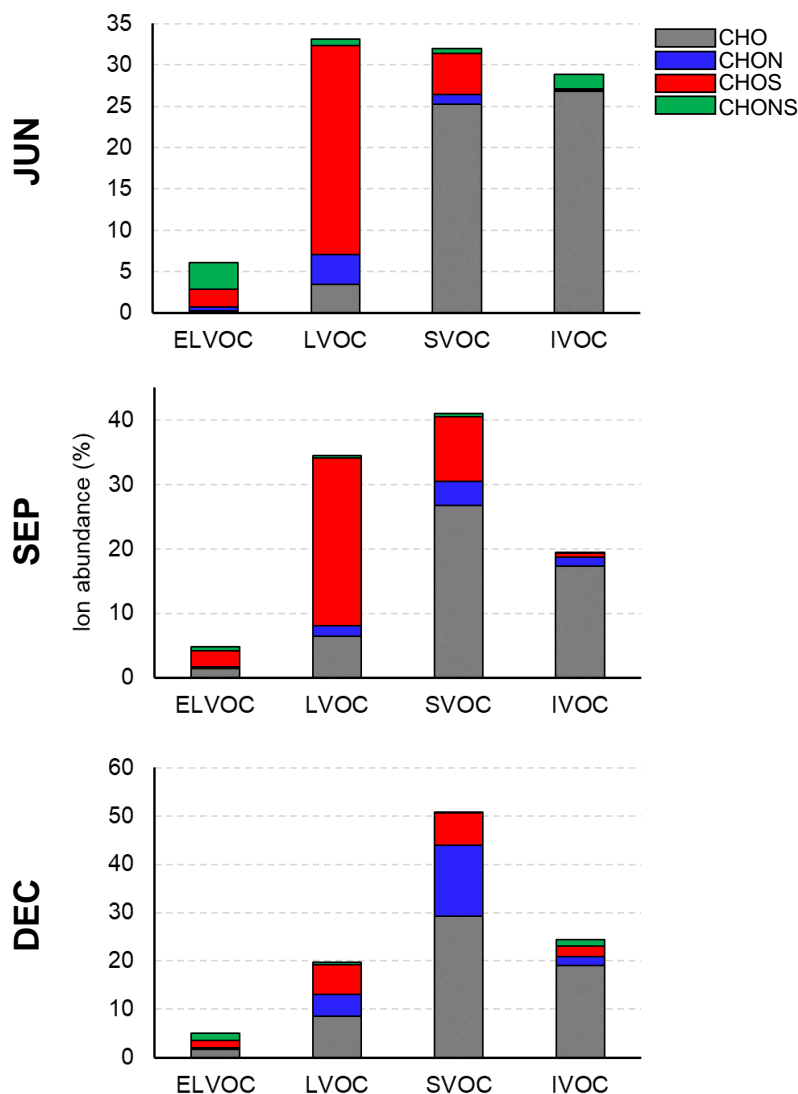
Figure 7. Compound class volatility distributions calculated for each seasonal period. Ion abundance (%) is relative to each sample.

volatility empirically by studying thermal desorption characteristics. The volatility and abundance of isoprene organosulfates observed in the study imply that these species are likely key contributors to UAP growth in the region. In addition to isoprene-

355 derived species, other CHOS molecules likely contribute significantly as well, as many of the individual species are classified as either LVOC or ELVOC ($C_0 < 3 \times 10^{-4}$) (Fig. S10). Given that easterly winds were dominant during the sampling periods (Fig. 3A), a key source of sulfate is likely oxidation of dimethylsulfide (DMS), a VOC associated with marine environments (Andreae and Raemdonck, 1983). The Amazon ecosystem itself has also been identified as another source of DMS, with emissions from plants and soils shown to be strongly dependant on light and temperature (Jardine et al., 2015). In addition

360 to DMS, regional sulfate production and thus UAP growth is likely highly sensitive to any contributions from SO_2 emission

sources such as biomass burning and fossil fuel combustion on land and at sea (Andreae, 2019; Lee et al., 2011). The abundant

biomass burning-related species including $C_7H_7O_4N$ (C_0 = 296 μg/m^3) and $C_7H_{12}O_7$ (C_0 = 7.6 μg/m^3) fall into the SVOC

fraction, contributing to the dominance of this fraction in DEC. Also contributing to the SVOC fraction are several MT SOA

markers such as MBTCA ($C_8H_{12}O_6$, C_0 = 94 μg/m^3) and C_{9-10} monomer species. CHO monomers with $C_{<8}$ associated with

365 monoterpene and isoprene oxidation are generally classified here as intermediate volatility species (IVOC) ($300 < C_0 < 3 \times$

10^6 μg/m^3). Though functional group elucidation may prove them to have a lower volatility due to the suspected abundance of

hydroxyl moieties (Donahue et al., 2011), the PBOA sugar markers are classified here as either SVOC (glucose and mannitol) or

IVOC (arabitol) species. In general, the molecular volatility distributions taken together with the size distribution data suggest

that the secondary UAPs measured here were likely nucleated elsewhere such as over the Atlantic ocean or the Amazon free

370 troposphere and what was sampled are mostly aged aerosol components ranging from low to intermediate volatility. UAPs

above nucleation sizes (>10 nm in diameter) are also likely contributed from other sources at the regional level such as biomass

burning in the dry season (SEP and DEC) and biological spore emissions in the late wet season (JUN).

5   Conclusions

UAPs collected from an eastern Amazon rainforest during three distinct seasonal periods exhibited compositional differences

375 that reflect seasonality in emission sources and aerosol molecular processing. Our observations suggest isoprene oxidation

chemistry is likely a key contributor to UAP composition in the eastern Amazon year-round, and that any regional perturbations

in isoprene and/or sulfate emission sources could have a significant impact on UAP formation and growth characteristics in

the future. Known markers for biological spore emissions were tentatively identified in UAPs with peak abundance observed

in the late wet season sample (JUN). To the best of our knowledge, this finding provides the first chemical evidence for the

380 influence of primary biogenic sources on UAP composition in the Amazon. To better assess this source's relative importance,

future measurements are needed to establish the prevalence of spore emission and fragmentation throughout the wet season and

in different regions of the Amazon. Secondary emission sources related to the oxidation of isoprene and monoterpenes appear

to contribute most to UAP composition during the peak dry season (SEP), aligning with the seasonal peak in VOC emissions

and solar radiation. In the late dry season (DEC), biomass burning appears to have a substantial impact on UAP composition,

385 as indicated by the abundance of tentatively identified species such as methyl-nitrocatechol and corroborated by MODIS fire

anomaly data. Future emission scenarios in which wildfire and agricultural burning events are more frequent could therefore

significantly alter regional UAP concentrations and growth characteristics during this time of year. Inasmuch as the Tapajós

rainforest is viewed as a model for the future of the Amazon (Cox et al., 2000), our study provides evidence that this source

will likely have increasing influence on UAP emissions in other regions such as Central Amazonia as well.

390 Reflecting the differences observed in the distribution of suspected marker species, seasonal changes in the properties of all

UAP molecular constituents were also apparent. Compared to those observed in the late wet season, CHO and CHON organics

detected in the dry season were more oxidized and unsaturated, suggesting a difference in the extent of aerosol processing

17

such as photochemical aging. Examining the distribution of molecular volatilities reveals that while a strong presence of low volatility species were found in the late wet and peak dry season due to the abundance of isoprene-derived organosulfates,
395 semi-volatile species likely emitted from biomass burning dominate the volatility distribution in the late dry season. Although the strong presence of low volatility organosulfates suggests that many of the sampled UAPs formed via sulfuric acid nucleation occurring to the east of the site, it is unclear whether semi-volatile species contributed from biomass burning condensed on these seeded particles or were emitted/formed by a separate mechanism. Similarly, it is unclear what fraction of observed semi-volatile BVOC oxidation products contributed to condensational growth of seeded particles near the surface or nucleated
400 new particles in the upper atmosphere. Future studies on the mixing state of Amazon UAPs would help us more quantitatively understand how the identified emission sources fit in the formation and growth history of new particles in the region. Regardless, it is clear both from the year-round abundance of sulfated species as well as the seasonal abundance of biomass burning markers in UAPs that human activity is likely already playing a role in formation and growth processes, and will indeed have greater influence in a probable future.

405 *Data availability.* Data are publicly available and are archived at https://doi.org/10.5061/dryad.k6djh9wgb (Smith, 2024)

Author contributions. JNS and JT secured funding, conceived research concept and made on-site measurements. JNS and HSG retrieved samples and analyzed size distribution data. AET analyzed samples and visualized data under supervision of JNS. AET prepared the manuscript with contributions from all authors.

Competing interests. The authors declare that they have no conflict of interests.

References

Allan, J. D., Morgan, W. T., Darbyshire, E., Flynn, M. J., Williams, P. I., Oram, D. E., Artaxo, P., Brito, J., Lee, J. D., and Coe, H.: Airborne observations of IEPOX-derived isoprene SOA in the Amazon during SAMBBA, Atmospheric Chemistry and Physics, 14, 11 393–11 407,
420   https://doi.org/10.5194/acp-14-11393-2014, 2014.

Allen, J., Oberdorster, G., Morris-Schaffer, K., Wong, C., Klocke, C., Sobolewski, M., Conrad, K., Mayer-Proschel, M., and Cory-Slechta, D.: Developmental neurotoxicity of inhaled ambient ultrafine particle air pollution: Parallels with neuropathological and behavioral features of autism and other neurodevelopmental disorders, NeuroToxicology, 59, 140–154, https://doi.org/10.1016/j.neuro.2015.12.014, 2017.

Alves, E. G., Jardine, K., Tota, J., Jardine, A., Yãnez-Serrano, A. M., Karl, T., Tavares, J., Nelson, B., Gu, D., Stavrakou, T., Martin, S.,
425   Artaxo, P., Manzi, A., and Guenther, A.: Seasonality of isoprenoid emissions from a primary rainforest in central Amazonia, Atmospheric Chemistry and Physics, 16, 3903–3925, https://doi.org/10.5194/acp-16-3903-2016, 2016.

Alves, E. G., Taylor, T., Robin, M., Oliveira, D. P., Schietti, J., Júnior, S. D., Zannoni, N., Williams, J., Hartmann, C., Gonçalves, J. F. C., Schöngart, J., Wittmann, F., and Piedade, M. T. F.: Seasonal shifts in isoprenoid emission composition from three hyperdominant tree species in central Amazonia, Plant Biology, 24, 721–733, https://doi.org/10.1111/plb.13419, 2022.

430 Andreae, M. O.: Emission of trace gases and aerosols from biomass burning – an updated assessment, Atmospheric Chemistry and Physics, 19, 8523–8546, https://doi.org/10.5194/acp-19-8523-2019, 2019.

Andreae, M. O. and Raemdonck, H.: Dimethyl Sulfide in the Surface Ocean and the Marine Atmosphere: A Global View, Science, 221, 744–747, https://doi.org/10.1126/science.221.4612.744, 1983.

Andreae, M. O., Rosenfeld, D., Artaxo, P., Costa, A. A., Frank, G. P., Longo, K. M., and Silva-Dias, M. A. F.: Smoking Rain Clouds over
435   the Amazon, Science, 303, 1337–1342, https://doi.org/10.1126/science.1092779, 2004.

Andreae, M. O., Afchine, A., Albrecht, R., Holanda, B. A., Artaxo, P., Barbosa, H. M. J., Borrmann, S., Cecchini, M. A., Costa, A., Dollner, M., Fütterer, D., Järvinen, E., Jurkat, T., Klimach, T., Konemann, T., Knote, C., Krämer, M., Krisna, T., Machado, L. A. T., Mertes, S., Minikin, A., Pöhlker, C., Pöhlker, M. L., Pöschl, U., Rosenfeld, D., Sauer, D., Schlager, H., Schnaiter, M., Schneider, J., Schulz, C., Spanu, A., Sperling, V. B., Voigt, C., Walser, A., Wang, J., Weinzierl, B., Wendisch, M., and Ziereis, H.: Aerosol characteristics and particle pro-
440   duction in the upper troposphere over the Amazon Basin, Atmospheric Chemistry and Physics, 18, 921–961, https://doi.org/10.5194/acp-18-921-2018, 2018.

Andreae, M. O., Andreae, T. W., Ditas, F., and Pöhlker, C.: Frequent new particle formation at remote sites in the subboreal forest of North America, Atmospheric Chemistry and Physics, 22, 2487–2505, https://doi.org/10.5194/acp-22-2487-2022, 2022.

Armstrong, N. C., Chen, Y., Cui, T., Zhang, Y., Christensen, C., Zhang, Z., Turpin, B. J., Chan, M. N., Gold, A., Ault, A. P., and Surratt, J. D.:
445   Isoprene Epoxydiol-Derived Sulfated and Nonsulfated Oligomers Suppress Particulate Mass Loss during Oxidative Aging of Secondary Organic Aerosol, Environmental Science Technology, 56, 16 611–16 620, https://doi.org/10.1021/acs.est.2c03200, 2022.

Aschmann, S. M. and Atkinson, R.: Formation Yields of Methyl Vinyl Ketone and Methacrolein from the Gas-Phase Reaction of O3 with Isoprene, Environmental Science Technology, 28, 1539–1542, https://doi.org/10.1021/es00057a025, 1994.

Attygalle, A. B., García-Rubio, S., Ta, J., and Meinwald, J.: Collisionally-induced dissociation mass spectra of organic sulfate anions, Journal
450   of the Chemical Society, Perkin Transactions 2, pp. 498–506, https://doi.org/10.1039/b009019k, 2001.

Baboomian, V. J., Crescenzo, G. V., Huang, Y., Mahrt, F., Shiraiwa, M., Bertram, A. K., and Nizkorodov, S. A.: Sunlight can convert atmospheric aerosols into a glassy solid state and modify their environmental impacts, Proceedings of the National Academy of Sciences, 119, https://doi.org/10.1073/pnas.2208121119, 2022.

Barket, D. J., Grossenbacher, J. W., Hurst, J. M., Shepson, P. B., Olszyna, K., Thornberry, T., Carroll, M. A., Roberts, J., Stroud, C.,
455   Bottenheim, J., and Biesenthal, T.: A study of the NO x dependence of isoprene oxidation, Journal of Geophysical Research: Atmospheres,
       109, https://doi.org/10.1029/2003JD003965, 2004.

Bauer, H., Claeys, M., Vermeylen, R., Schueller, E., Weinke, G., Berger, A., and Puxbaum, H.: Arabitol and mannitol as tracers for the
       quantification of airborne fungal spores, Atmospheric Environment, 42, 588–593, https://doi.org/10.1016/j.atmosenv.2007.10.013, 2008.

Bianchi, F., Kurtén, T., Riva, M., Mohr, C., Rissanen, M. P., Roldin, P., Berndt, T., Crounse, J. D., Wennberg, P. O., Mentel, T. F., Wildt,
460   J., Junninen, H., Jokinen, T., Kulmala, M., Worsnop, D. R., Thornton, J. A., Donahue, N., Kjaergaard, H. G., and Ehn, M.: Highly
       Oxygenated Organic Molecules (HOM) from Gas-Phase Autoxidation Involving Peroxy Radicals: A Key Contributor to Atmospheric
       Aerosol, https://doi.org/10.1021/acs.chemrev.8b00395, 2019.

Brock, C. A., Hamill, P., Wilson, J. C., Jonsson, H. H., and Chan, K. R.: Particle Formation in the Upper Tropical Troposphere: A Source of
       Nuclei for the Stratospheric Aerosol, Science, 270, 1650–1653, https://doi.org/10.1126/science.270.5242.1650, 1995.

465   Calderón-Garcidueñas, L. and Ayala, A.: Air Pollution, Ultrafine Particles, and Your Brain: Are Combustion Nanoparticle Emissions and
       Engineered Nanoparticles Causing Preventable Fatal Neurodegenerative Diseases and Common Neuropsychiatric Outcomes?, Environ-
       mental Science Technology, 56, 6847–6856, https://doi.org/10.1021/acs.est.1c04706, 2022.

Chen, Q., Farmer, D. K., Rizzo, L. V., Pauliquevis, T., Kuwata, M., Karl, T. G., Guenther, A., Allan, J. D., Coe, H., Andreae, M. O., Pöschl,
       U., Jimenez, J. L., Artaxo, P., and Martin, S. T.: Submicron particle mass concentrations and sources in the Amazonian wet season
470   (AMAZE-08), Atmospheric Chemistry and Physics, 15, 3687–3701, https://doi.org/10.5194/acp-15-3687-2015, 2015.

China, S., Wang, B., Weis, J., Rizzo, L., Brito, J., Cirino, G. G., Kovarik, L., Artaxo, P., Gilles, M. K., and Laskin, A.: Ruptur-
       ing of Biological Spores As a Source of Secondary Particles in Amazonia, Environmental Science Technology, 50, 12 179–12 186,
       https://doi.org/10.1021/acs.est.6b02896, 2016.

Claeys, M., Graham, B., Vas, G., Wang, W., Vermeylen, R., Pashynska, V., Cafmeyer, J., Guyon, P., Andreae, M. O., Artaxo, P.,
475   and Maenhaut, W.: Formation of Secondary Organic Aerosols Through Photooxidation of Isoprene, Science, 303, 1173–1176,
       https://doi.org/10.1126/science.1092805, 2004.

Claeys, M., Szmigielski, R., Kourtchev, I., der Veken, P. V., Vermeylen, R., Maenhaut, W., Jaoui, M., Kleindienst, T. E., Lewandowski, M.,
       Offenberg, J. H., and Edney, E. O.: Hydroxydicarboxylic Acids: Markers for Secondary Organic Aerosol from the Photooxidation of
       α-Pinene, Environmental Science Technology, 41, 1628–1634, https://doi.org/10.1021/es0620181, 2007.

480   Cox, P. M., Betts, R. A., Jones, C. D., Spall, S. A., and Totterdell, I. J.: Acceleration of global warming due to carbon-cycle feedbacks in a
       coupled climate model, Nature, 408, 184–187, https://doi.org/10.1038/35041539, 2000.

da Rocha, H. R., Manzi, A. O., Cabral, O. M., Miller, S. D., Goulden, M. L., Saleska, S. R., R.-Coupe, N., Wofsy, S. C., Borma, L. S.,
       Artaxo, P., Vourlitis, G., Nogueira, J. S., Cardoso, F. L., Nobre, A. D., Kruijt, B., Freitas, H. C., von Randow, C., Aguiar, R. G., and Maia,
       J. F.: Patterns of water and heat flux across a biome gradient from tropical forest to savanna in Brazil, Journal of Geophysical Research:
485   Biogeosciences, 114, https://doi.org/10.1029/2007JG000640, 2009.

Dada, L., Chellapermal, R., Mazon, S. B., Paasonen, P., Lampilahti, J., Manninen, H. E., Junninen, H., Petäjä, T., Kerminen, V.-M., and Kul-
       mala, M.: Refined classification and characterization of atmospheric new-particle formation events using air ions, Atmospheric Chemistry
       and Physics, 18, 17 883–17 893, https://doi.org/10.5194/acp-18-17883-2018, 2018.

Dal Maso, M., Sogacheva, L., Anisimov, M. P., Arshinov, M., Baklanov, A., Belan, B., Khodzer, T. V., Obolkin, V. A., Staroverova, A.,
490   Vlasov, A., et al.: Aerosol particle formation events at two Siberian stations inside the boreal forest, 13, 81–92, 2008.

de Sá, S. S., Rizzo, L. V., Palm, B. B., Campuzano-Jost, P., Day, D. A., Yee, L. D., Wernis, R., Isaacman-VanWertz, G., Brito, J., Carbone, S., Liu, Y. J., Sedlacek, A., Springston, S., Goldstein, A. H., Barbosa, H. M. J., Alexander, M. L., Artaxo, P., Jimenez, J. L., and Martin, S. T.: Contributions of biomass-burning, urban, and biogenic emissions to the concentrations and light-absorbing properties of particulate matter in central Amazonia during the dry season, Atmospheric Chemistry and Physics, 19, https://doi.org/10.5194/acp-19-7973-2019, 2019.

Donahue, N. M., Epstein, S. A., Pandis, S. N., and Robinson, A. L.: A two-dimensional volatility basis set: 1. organic-aerosol mixing thermodynamics, Atmospheric Chemistry and Physics, 11, 3303–3318, https://doi.org/10.5194/acp-11-3303-2011, 2011.

Dunne, E. M., Gordon, H., Kürten, A., Almeida, J., Duplissy, J., Williamson, C., Ortega, I. K., Pringle, K. J., Adamov, A., Baltensperger, U., Barmet, P., Benduhn, F., Bianchi, F., Breitenlechner, M., Clarke, A., Curtius, J., Dommen, J., Donahue, N. M., Ehrhart, S., Flagan, R. C., Franchin, A., Guida, R., Hakala, J., Hansel, A., Heinritzi, M., Jokinen, T., Kangasluoma, J., Kirkby, J., Kulmala, M., Kupc, A., Lawler, M. J., Lehtipalo, K., Makhmutov, V., Mann, G., Mathot, S., Merikanto, J., Miettinen, P., Nenes, A., Onnela, A., Rap, A., Reddington, C. L. S., Riccobono, F., Richards, N. A. D., Rissanen, M. P., Rondo, L., Sarnela, N., Schobesberger, S., Sengupta, K., Simon, M., Sipilä, M., Smith, J. N., Stozkhov, Y., Tomé, A., Tröstl, J., Wagner, P. E., Wimmer, D., Winkler, P. M., Worsnop, D. R., and Carslaw, K. S.: Global atmospheric particle formation from CERN CLOUD measurements, Science, 354, 1119–1124, https://doi.org/10.1126/science.aaf2649, 2016.

Ehn, M., Thornton, J. A., Kleist, E., Sipilä, M., Junninen, H., Pullinen, I., Springer, M., Rubach, F., Tillmann, R., Lee, B., Lopez-Hilfiker, F., Andres, S., Acir, I.-H., Rissanen, M., Jokinen, T., Schobesberger, S., Kangasluoma, J., Kontkanen, J., Nieminen, T., Kurtén, T., Nielsen, L. B., Jørgensen, S., Kjaergaard, H. G., Canagaratna, M., Maso, M. D., Berndt, T., Petäjä, T., Wahner, A., Kerminen, V.-M., Kulmala, M., Worsnop, D. R., Wildt, J., and Mentel, T. F.: A large source of low-volatility secondary organic aerosol, Nature, 506, 476–479, https://doi.org/10.1038/nature13032, 2014.

Ekman, A. M. L., Krejci, R., Engström, A., Ström, J., de Reus, M., Williams, J., and Andreae, M. O.: Do organics contribute to small particle formation in the Amazonian upper troposphere?, Geophysical Research Letters, 35, https://doi.org/10.1029/2008GL034970, 2008.

Fan, J., Rosenfeld, D., Zhang, Y., Giangrande, S. E., Li, Z., Machado, L. A. T., Martin, S. T., Yang, Y., Wang, J., Artaxo, P., Barbosa, H. M. J., Braga, R. C., Comstock, J. M., Feng, Z., Gao, W., Gomes, H. B., Mei, F., Pöhlker, C., Pöhlker, M. L., Pöschl, U., and de Souza, R. A. F.: Substantial convection and precipitation enhancements by ultrafineaerosol particles, Science, 359, 411–418, https://doi.org/10.1126/science.aan8461, 2018.

Fernandez, A. E., Lewis, G. S., and Hering, S. V.: Design and Laboratory Evaluation of a Sequential Spot Sampler for Time-Resolved Measurement of Airborne Particle Composition, Aerosol Science and Technology, 48, https://doi.org/10.1080/02786826.2014.911409, 2014.

Flores, B. M., Montoya, E., Sakschewski, B., Nascimento, N., Staal, A., Betts, R. A., Levis, C., Lapola, D. M., Esquível-Muelbert, A., Jakovac, C., Nobre, C. A., Oliveira, R. S., Borma, L. S., Nian, D., Boers, N., Hecht, S. B., ter Steege, H., Arieira, J., Lucas, I. L., Berenguer, E., Marengo, J. A., Gatti, L. V., Mattos, C. R. C., and Hirota, M.: Critical transitions in the Amazon forest system, Nature, 626, 555–564, https://doi.org/10.1038/s41586-023-06970-0, 2024.

Giglio, L., Boschetti, L., Roy, D. P., Humber, M. L., and Justice, C. O.: The Collection 6 MODIS burned area mapping algorithm and product, Remote Sensing of Environment, 217, 72–85, https://doi.org/10.1016/j.rse.2018.08.005, 2018.

Glasius, M., Bering, M. S., Yee, L. D., de Sá, S. S., Isaacman-VanWertz, G., Wernis, R. A., Barbosa, H. M. J., Alexander, M. L., Palm, B. B., Hu, W., Campuzano-Jost, P., Day, D. A., Jimenez, J. L., Shrivastava, M., Martin, S. T., and Goldstein, A. H.: Organosul-

fates in aerosols downwind of an urban region in central Amazon, Environmental Science: Processes Impacts, 20, 1546–1558, https://doi.org/10.1039/C8EM00413G, 2018.

530 Glicker, H. S., Lawler, M. J., Ortega, J., de Sá, S. S., Martin, S. T., Artaxo, P., Bustillos, O. V., de Souza, R., Tota, J., Carlton, A., and Smith, J. N.: Chemical composition of ultrafine aerosol particles in central Amazonia during the wet season, Atmospheric Chemistry and Physics, 19, https://doi.org/10.5194/acp-19-13053-2019, 2019.

Gordon, H., Kirkby, J., Baltensperger, U., Bianchi, F., Breitenlechner, M., Curtius, J., Dias, A., Dommen, J., Donahue, N. M., Dunne, E. M., Duplissy, J., Ehrhart, S., Flagan, R. C., Frege, C., Fuchs, C., Hansel, A., Hoyle, C. R., Kulmala, M., Kürten, A., Lehtipalo, K., Makhmutov,

535 V., Molteni, U., Rissanen, M. P., Stozkhov, Y., Tröstl, J., Tsagkogeorgas, G., Wagner, R., Williamson, C., Wimmer, D., Winkler, P. M., Yan, C., and Carslaw, K. S.: Causes and importance of new particle formation in the present-day and preindustrial atmospheres, Journal of Geophysical Research: Atmospheres, 122, 8739–8760, https://doi.org/10.1002/2017JD026844, 2017.

Guenther, A. B., Jiang, X., Heald, C. L., Sakulyanontvittaya, T., Duhl, T., Emmons, L. K., and Wang, X.: The Model of Emissions of Gases and Aerosols from Nature version 2.1 (MEGAN2.1): an extended and updated framework for modeling biogenic emissions, Geoscientific

540 Model Development, 5, 1471–1492, https://doi.org/10.5194/gmd-5-1471-2012, 2012.

Hersbach, H., Bell, B., Berrisford, P., Biavati, G., Horányi, A., Muñoz Sabater, J., Nicolas, J., Peubey, C., Radu, R., Rozum, I., Schepers, D., Simmons, A., Soci, C., Dee, D., and Thépaut, J.-N.: ERA5 hourly data on single levels from 1940 to present. Copernicus Climate Change Service (C3S) Climate Data Store (CDS), Accessed 5/13/2024, https://doi.org/10.24381/cds.adbb2d47, 2023.

Hodshire, A. L., Palm, B. B., Alexander, M. L., Bian, Q., Campuzano-Jost, P., Cross, E. S., Day, D. A., de Sá, S. S., Guenther, A. B.,

545 Hansel, A., Hunter, J. F., Jud, W., Karl, T., Kim, S., Kroll, J. H., Park, J.-H., Peng, Z., Seco, R., Smith, J. N., Jimenez, J. L., and Pierce, J. R.: Constraining nucleation, condensation, and chemistry in oxidation flow reactors using size-distribution measurements and aerosol microphysical modeling, Atmospheric Chemistry and Physics, 18, 12 433–12 460, https://doi.org/10.5194/acp-18-12433-2018, 2018.

Huffman, J. A., Prenni, A. J., DeMott, P. J., Pöhlker, C., Mason, R. H., Robinson, N. H., Fröhlich-Nowoisky, J., Tobo, Y., Després, V. R., Garcia, E., Gochis, D. J., Harris, E., Müller-Germann, I., Ruzene, C., Schmer, B., Sinha, B., Day, D. A., Andreae, M. O., Jimenez, J. L.,

550 Gallagher, M., Kreidenweis, S. M., Bertram, A. K., and Pöschl, U.: High concentrations of biological aerosol particles and ice nuclei during and after rain, Atmospheric Chemistry and Physics, 13, 6151–6164, https://doi.org/10.5194/acp-13-6151-2013, 2013.

Iinuma, Y., Böge, O., Gräfe, R., and Herrmann, H.: Methyl-Nitrocatechols: Atmospheric Tracer Compounds for Biomass Burning Secondary Organic Aerosols, Environmental Science Technology, 44, https://doi.org/10.1021/es102938a, 2010.

Isaacman-VanWertz, G., Yee, L. D., Kreisberg, N. M., Wernis, R., Moss, J. A., Hering, S. V., de Sá, S. S., Martin, S. T., Alexander, M. L.,

555 Palm, B. B., Hu, W., Campuzano-Jost, P., Day, D. A., Jimenez, J. L., Riva, M., Surratt, J. D., Viegas, J., Manzi, A., Edgerton, E., Baumann, K., Souza, R., Artaxo, P., and Goldstein, A. H.: Ambient Gas-Particle Partitioning of Tracers for Biogenic Oxidation, Environmental Science Technology, 50, 9952–9962, https://doi.org/10.1021/acs.est.6b01674, 2016.

Jaitly, N., Mayampurath, A., Littlefield, K., Adkins, J. N., Anderson, G. A., and Smith, R. D.: Decon2LS: An open-source software package for automated processing and visualization of high resolution mass spectrometry data, BMC Bioinformatics, 10, 87,

560 https://doi.org/10.1186/1471-2105-10-87, 2009.

Jaoui, M., Szmigielski, R., Nestorowicz, K., Kolodziejczyk, A., Sarang, K., Rudzinski, K. J., Konopka, A., Bulska, E., Lewandowski, M., and Kleindienst, T. E.: Organic Hydroxy Acids as Highly Oxygenated Molecular (HOM) Tracers for Aged Isoprene Aerosol, Environmental Science Technology, 53, https://doi.org/10.1021/acs.est.9b05075, 2019.

Jardine, K., Yañez-Serrano, A. M., Williams, J., Kunert, N., Jardine, A., Taylor, T., Abrell, L., Artaxo, P., Guenther, A., Hewitt,

565 C. N., House, E., Florentino, A. P., Manzi, A., Higuchi, N., Kesselmeier, J., Behrendt, T., Veres, P. R., Derstroff, B., Fuentes,

J. D., Martin, S. T., and Andreae, M. O.: Dimethyl sulfide in the Amazon rain forest, Global Biogeochemical Cycles, 29, 19–32, https://doi.org/10.1002/2014GB004969, 2015.

Jenkins, B. M., Jones, A. D., Turn, S. Q., and Williams, R. B.: Emission Factors for Polycyclic Aromatic Hydrocarbons from Biomass Burning, Environmental Science Technology, 30, 2462–2469, https://doi.org/10.1021/es950699m, 1996.

570 Jiang, H., Carena, L., He, Y., Wang, Y., Zhou, W., Yang, L., Luan, T., Li, X., Brigante, M., Vione, D., and Gligorovski, S.: Photosensitized Degradation of DMSO Initiated by PAHs at the Air-Water Interface, as an Alternative Source of Organic Sulfur Compounds to the Atmosphere, Journal of Geophysical Research: Atmospheres, 126, https://doi.org/10.1029/2021JD035346, 2021.

Jiang, H., He, Y., Wang, Y., Li, S., Jiang, B., Carena, L., Li, X., Yang, L., Luan, T., Vione, D., and Gligorovski, S.: Formation of organic sulfur compounds through SO2-initiated photochemistry of PAHs and dimethylsulfoxide at the air-water interface, Atmospheric Chemistry and

575 Physics, 22, 4237–4252, https://doi.org/10.5194/acp-22-4237-2022, 2022.

Kahnt, A., Iinuma, Y., Blockhuys, F., Mutzel, A., Vermeylen, R., Kleindienst, T. E., Jaoui, M., Offenberg, J. H., Lewandowski, M., Böge, O., Herrmann, H., Maenhaut, W., and Claeys, M.: 2-Hydroxyterpenylic Acid: An Oxygenated Marker Compound for α-Pinene Secondary Organic Aerosol in Ambient Fine Aerosol, Environmental Science Technology, 48, 4901–4908, https://doi.org/10.1021/es500377d, 2014.

Karl, T. G., Christian, T. J., Yokelson, R. J., Artaxo, P., Hao, W. M., and Guenther, A.: The Tropical Forest and Fire Emissions Experi-
580 ment: method evaluation of volatile organic compound emissions measured by PTR-MS, FTIR, and GC from tropical biomass burning, Atmospheric Chemistry and Physics, 7, 5883–5897, https://doi.org/10.5194/acp-7-5883-2007, 2007.

Kong, X., Salvador, C. M., Carlsson, S., Pathak, R., Davidsson, K. O., Breton, M. L., Gaita, S. M., Mitra, K., Åsa M. Hallquist, Hallquist, M., and Pettersson, J. B.: Molecular characterization and optical properties of primary emissions from a residential wood burning boiler, Science of The Total Environment, 754, 142 143, https://doi.org/10.1016/j.scitotenv.2020.142143, 2021.

585 Kourtchev, I., Godoi, R. H. M., Connors, S., Levine, J. G., Archibald, A. T., Godoi, A. F. L., Paralovo, S. L., Barbosa, C. G. G., Souza, R. A. F., Manzi, A. O., Seco, R., Sjostedt, S., Park, J.-H., Guenther, A., Kim, S., Smith, J., Martin, S. T., and Kalberer, M.: Molecular composition of organic aerosols in central Amazonia: an ultra-high-resolution mass spectrometry study, Atmospheric Chemistry and Physics, 16, https://doi.org/10.5194/acp-16-11899-2016, 2016.

Kourtchev, I., Szeto, P., O'Connor, I., Popoola, O. A. M., Maenhaut, W., Wenger, J., and Kalberer, M.: Comparison of Heated Electro-
590 spray Ionization and Nanoelectrospray Ionization Sources Coupled to Ultra-High-Resolution Mass Spectrometry for Analysis of Highly Complex Atmospheric Aerosol Samples, Analytical Chemistry, 92, 8396–8403, https://doi.org/10.1021/acs.analchem.0c00971, 2020.

Krechmer, J. E., Coggon, M. M., Massoli, P., Nguyen, T. B., Crounse, J. D., Hu, W., Day, D. A., Tyndall, G. S., Henze, D. K., Rivera-Rios, J. C., Nowak, J. B., Kimmel, J. R., Mauldin, R. L., Stark, H., Jayne, J. T., Sipilä, M., Junninen, H., Clair, J. M. S., Zhang, X., Feiner, P. A., Zhang, L., Miller, D. O., Brune, W. H., Keutsch, F. N., Wennberg, P. O., Seinfeld, J. H., Worsnop, D. R., Jimenez, J. L., and Canagaratna,
595 M. R.: Formation of Low Volatility Organic Compounds and Secondary Organic Aerosol from Isoprene Hydroxyhydroperoxide Low-NO Oxidation, Environmental Science Technology, 49, 10 330–10 339, https://doi.org/10.1021/acs.est.5b02031, 2015.

Kroll, J. H., Donahue, N. M., Jimenez, J. L., Kessler, S. H., Canagaratna, M. R., Wilson, K. R., Altieri, K. E., Mazzoleni, L. R., Wozniak, A. S., Bluhm, H., Mysak, E. R., Smith, J. D., Kolb, C. E., and Worsnop, D. R.: Carbon oxidation state as a metric for describing the chemistry of atmospheric organic aerosol, Nature Chemistry, 3, https://doi.org/10.1038/nchem.948, 2011.

600 Kuang, B. Y., Lin, P., Hu, M., and Yu, J. Z.: Aerosol size distribution characteristics of organosulfates in the Pearl River Delta region, China, Atmospheric Environment, 130, 23–35, https://doi.org/10.1016/j.atmosenv.2015.09.024, 2016.

Kubátová, A., Vermeylen, R., Claeys, M., Cafmeyer, J., Maenhaut, W., Roberts, G., and Artaxo, P.: Carbonaceous aerosol character-
ization in the Amazon basin, Brazil: novel dicarboxylic acids and related compounds, Atmospheric Environment, 34, 5037–5051,
https://doi.org/10.1016/S1352-2310(00)00320-4, 2000.

605 Langford, B., House, E., Valach, A., Hewitt, C. N., Artaxo, P., Barkley, M. P., Brito, J., Carnell, E., Davison, B., MacKenzie, A. R., Marais,
E. A., Newland, M. J., Rickard, A. R., Shaw, M. D., Yáñez-Serrano, A. M., and Nemitz, E.: Seasonality of isoprene emissions and
oxidation products above the remote Amazon, Environmental Science: Atmospheres, 2, 230–240, https://doi.org/10.1039/D1EA00057H,
2022.

Lawler, M. J., Draper, D. C., and Smith, J. N.: Atmospheric fungal nanoparticle bursts, Science Advances, 6,
610 https://doi.org/10.1126/sciadv.aax9051, 2020.

Lawson, D. R. and Winchester, J. W.: Sulfur, potassium, and phosphorus associations in aerosols from South American tropical rain forests,
Journal of Geophysical Research: Oceans, 84, 3723–3727, https://doi.org/10.1029/JC084iC07p03723, 1979.

Lee, C., Martin, R. V., van Donkelaar, A., Lee, H., Dickerson, R. R., Hains, J. C., Krotkov, N., Richter, A., Vinnikov, K., and Schwab, J. J.: SO
2 emissions and lifetimes: Estimates from inverse modeling using in situ and global, space-based (SCIAMACHY and OMI) observations,
615 Journal of Geophysical Research, 116, D06 304, https://doi.org/10.1029/2010JD014758, 2011.

Leppla, D., Zannoni, N., Kremper, L., Williams, J., Pöhlker, C., Sá, M., Solci, M. C., and Hoffmann, T.: Varying chiral ratio of pinic acid
enantiomers above the Amazon rainforest, Atmospheric Chemistry and Physics, 23, 809–820, https://doi.org/10.5194/acp-23-809-2023,
2023.

Lewis, D. H. and Smith, D. C.: Sugar Alcohols (Polyols) in Fungi and Green Plants. I. Distribution, Physiology and Metabolism, The New
620 Phytologist, 66, 143–184, http://www.jstor.org/stable/2430328, 1967.

Li, H., Xu, D., Li, H., Wu, Y., Cheng, Y., Chen, Z., Yin, G., Wang, W., Ge, Y., Niu, Y., Liu, C., Cai, J., Kan, H., Yu, D., and Chen, R.: Exposure
to ultrafine particles and oral flora, respiratory function, and biomarkers of inflammation: A panel study in children, Environmental
Pollution, 273, 116 489, https://doi.org/10.1016/j.envpol.2021.116489, 2021.

Li, Y., Pöschl, U., and Shiraiwa, M.: Molecular corridors and parameterizations of volatility in the chemical evolution of organic aerosols,
625 Atmospheric Chemistry and Physics, 16, 3327–3344, https://doi.org/10.5194/acp-16-3327-2016, 2016.

Liao, J., Froyd, K. D., Murphy, D. M., Keutsch, F. N., Yu, G., Wennberg, P. O., Clair, J. M. S., Crounse, J. D., Wisthaler, A., Mikoviny, T.,
Jimenez, J. L., Campuzano-Jost, P., Day, D. A., Hu, W., Ryerson, T. B., Pollack, I. B., Peischl, J., Anderson, B. E., Ziemba, L. D., Blake,
D. R., Meinardi, S., and Diskin, G.: Airborne measurements of organosulfates over the continental U.S., Journal of Geophysical Research:
Atmospheres, 120, 2990–3005, https://doi.org/10.1002/2014JD022378, 2015.

630 Liu, J., D'Ambro, E. L., Lee, B. H., Lopez-Hilfiker, F. D., Zaveri, R. A., Rivera-Rios, J. C., Keutsch, F. N., Iyer, S., Kurten, T., Zhang, Z.,
Gold, A., Surratt, J. D., Shilling, J. E., and Thornton, J. A.: Efficient Isoprene Secondary Organic Aerosol Formation from a Non-IEPOX
Pathway, Environmental Science Technology, 50, 9872–9880, https://doi.org/10.1021/acs.est.6b01872, 2016a.

Liu, Y., Brito, J., Dorris, M. R., Rivera-Rios, J. C., Seco, R., Bates, K. H., Artaxo, P., Duvoisin, S., Keutsch, F. N., Kim, S., Gold-
stein, A. H., Guenther, A. B., Manzi, A. O., Souza, R. A. F., Springston, S. R., Watson, T. B., McKinney, K. A., and Martin,
635 S. T.: Isoprene photochemistry over the Amazon rainforest, Proceedings of the National Academy of Sciences, 113, 6125–6130,
https://doi.org/10.1073/pnas.1524136113, 2016b.

Liu, Y., Seco, R., Kim, S., Guenther, A. B., Goldstein, A. H., Keutsch, F. N., Springston, S. R., Watson, T. B., Artaxo, P., Souza, R.
A. F., McKinney, K. A., and Martin, S. T.: Isoprene photo-oxidation products quantify the effect of pollution on hydroxyl radicals over
Amazonia, Science Advances, 4, https://doi.org/10.1126/sciadv.aar2547, 2018.

640   Liu, Y. J., Herdlinger-Blatt, I., McKinney, K. A., and Martin, S. T.: Production of methyl vinyl ketone and methacrolein via the hydroperoxyl
pathway of isoprene oxidation, Atmospheric Chemistry and Physics, 13, 5715–5730, https://doi.org/10.5194/acp-13-5715-2013, 2013.

Lopez-Hilfiker, F. D., Mohr, C., D'Ambro, E. L., Lutz, A., Riedel, T. P., Gaston, C. J., Iyer, S., Zhang, Z., Gold, A., Surratt, J. D.,
Lee, B. H., Kurten, T., Hu, W., Jimenez, J., Hallquist, M., and Thornton, J. A.: Molecular Composition and Volatility of Or-
ganic Aerosol in the Southeastern U.S.: Implications for IEPOX Derived SOA, Environmental Science Technology, 50, 2200–2209,
645   https://doi.org/10.1021/acs.est.5b04769, 2016.

Mabato, B. R. G., Lyu, Y., Ji, Y., Li, Y. J., Huang, D. D., Li, X., Nah, T., Lam, C. H., and Chan, C. K.: Aqueous secondary organic aerosol
formation from the direct photosensitized oxidation of vanillin in the absence and presence of ammonium nitrate, Atmospheric Chemistry
and Physics, 22, 273–293, https://doi.org/10.5194/acp-22-273-2022, 2022.

Maclean, A. M., Smith, N. R., Li, Y., Huang, Y., Hettiyadura, A. P. S., Crescenzo, G. V., Shiraiwa, M., Laskin, A., Nizkorodov, S. A.,
650   and Bertram, A. K.: Humidity-Dependent Viscosity of Secondary Organic Aerosol from Ozonolysis of β-Caryophyllene: Measurements,
Predictions, and Implications, ACS Earth and Space Chemistry, 5, 305–318, https://doi.org/10.1021/acsearthspacechem.0c00296, 2021.

Martin, S. T., Andreae, M. O., Artaxo, P., Baumgardner, D., Chen, Q., Goldstein, A. H., Guenther, A., Heald, C. L., Mayol-Bracero,
O. L., McMurry, P. H., Pauliquevis, T., Pöschl, U., Prather, K. A., Roberts, G. C., Saleska, S. R., Dias, M. A. S., Spracklen,
D. V., Swietlicki, E., and Trebs, I.: Sources and properties of Amazonian aerosol particles, Reviews of Geophysics, 48, RG2002,
655   https://doi.org/10.1029/2008RG000280, 2010.

Merikanto, J., Spracklen, D. V., Mann, G. W., Pickering, S. J., and Carslaw, K. S.: Impact of nucleation on global CCN, Atmospheric
Chemistry and Physics, 9, 8601–8616, https://doi.org/10.5194/acp-9-8601-2009, 2009.

Murphy, B. N., Donahue, N. M., Robinson, A. L., and Pandis, S. N.: A naming convention for atmospheric organic aerosol, Atmospheric
Chemistry and Physics, 14, 5825–5839, https://doi.org/10.5194/acp-14-5825-2014, 2014.

660   Nassan, F. L., Wang, C., Kelly, R. S., Lasky-Su, J. A., Vokonas, P. S., Koutrakis, P., and Schwartz, J. D.: Ambient PM2.5
species and ultrafine particle exposure and their differential metabolomic signatures, Environment International, 151, 106 447,
https://doi.org/10.1016/j.envint.2021.106447, 2021.

Nguyen, T. B., Bates, K. H., Crounse, J. D., Schwantes, R. H., Zhang, X., Kjaergaard, H. G., Surratt, J. D., Lin, P., Laskin, A., Se-
infeld, J. H., and Wennberg, P. O.: Mechanism of the hydroxyl radical oxidation of methacryloyl peroxynitrate (MPAN) and its
665   pathway toward secondary organic aerosol formation in the atmosphere, Physical Chemistry Chemical Physics, 17, 17 914–17 926,
https://doi.org/10.1039/C5CP02001H, 2015.

Nirmalkar, J., Deb, M. K., Tsai, Y. I., and Deshmukh, D. K.: Arabitol and Mannitol as Tracer for Fungal Contribution to Size-Differentiated
Particulate Matter of Rural Atmospheric Aerosols, International Journal of Environmental Science and Development, 6, 460–463,
https://doi.org/10.7763/IJESD.2015.V6.637, 2015.

670   Nizkorodov, S. A., Laskin, J., and Laskin, A.: Molecular chemistry of organic aerosols through the application of high resolution mass
spectrometry, Physical Chemistry Chemical Physics, 13, https://doi.org/10.1039/c0cp02032j, 2011.

Nölscher, A. C., Yañez-Serrano, A. M., Wolff, S., de Araujo, A. C., Lavrič, J. V., Kesselmeier, J., and Williams, J.: Unexpected seasonality in
quantity and composition of Amazon rainforest air reactivity, Nature Communications, 7, 10 383, https://doi.org/10.1038/ncomms10383,
2016.

675   Olsen, J. V., Macek, B., Lange, O., Makarov, A., Horning, S., and Mann, M.: Higher-energy C-trap dissociation for peptide modification
analysis, Nature Methods, 4, 709–712, https://doi.org/10.1038/nmeth1060, 2007.

Palm, B. B., de Sá, S. S., Day, D. A., Campuzano-Jost, P., Hu, W., Seco, R., Sjostedt, S. J., Park, J.-H., Guenther, A. B., Kim, S., Brito, J., Wurm, F., Artaxo, P., Thalman, R., Wang, J., Yee, L. D., Wernis, R., Isaacman-VanWertz, G., Goldstein, A. H., Liu, Y., Springston, S. R., Souza, R., Newburn, M. K., Alexander, M. L., Martin, S. T., and Jimenez, J. L.: Secondary organic aerosol formation from ambient air in an
680   oxidation flow reactor in central Amazonia, Atmospheric Chemistry and Physics, 18, 467–493, https://doi.org/10.5194/acp-18-467-2018, 2018.

Paulot, F., Crounse, J. D., Kjaergaard, H. G., Kürten, A., Clair, J. M. S., Seinfeld, J. H., and Wennberg, P. O.: Unexpected Epoxide Formation in the Gas-Phase Photooxidation of Isoprene, Science, 325, 730–733, https://doi.org/10.1126/science.1172910, 2009.

Pfannerstill, E. Y., Reijrink, N. G., Edtbauer, A., Ringsdorf, A., Zannoni, N., Araújo, A., Ditas, F., Holanda, B. A., Sá, M. O., Tsokankunku,
685   A., Walter, D., Wolff, S., Lavrič, J. V., Pöhlker, C., Sörgel, M., and Williams, J.: Total OH reactivity over the Amazon rainforest: variability with temperature, wind, rain, altitude, time of day, season, and an overall budget closure, Atmospheric Chemistry and Physics, 21, 6231–6256, https://doi.org/10.5194/acp-21-6231-2021, 2021.

Pöhlker, C., Wiedemann, K. T., Sinha, B., Shiraiwa, M., Gunthe, S. S., Smith, M., Su, H., Artaxo, P., Chen, Q., Cheng, Y., Elbert, W., Gilles, M. K., Kilcoyne, A. L. D., Moffet, R. C., Weigand, M., Martin, S. T., Pöschl, U., and Andreae, M. O.: Biogenic Potassium Salt Particles
690   as Seeds for Secondary Organic Aerosol in the Amazon, Science, 337, 1075–1078, https://doi.org/10.1126/science.1223264, 2012.

Reis, G., Souza, S., Neto, H., Branches, R., Silva, R., Peres, L., Pinheiro, D., Lamy, K., Bencherif, H., and Portafaix, T.: Solar Ultraviolet Radiation Temporal Variability Analysis from 2-Year of Continuous Observation in an Amazonian City of Brazil, Atmosphere, 13, 1054, https://doi.org/10.3390/atmos13071054, 2022.

Rinne, H., Guenther, A., Greenberg, J., and Harley, P.: Isoprene and monoterpene fluxes measured above Amazonian rainforest and their
695   dependence on light and temperature, Atmospheric Environment, 36, 2421–2426, https://doi.org/10.1016/S1352-2310(01)00523-4, 2002.

Riva, M., Chen, Y., Zhang, Y., Lei, Z., Olson, N. E., Boyer, H. C., Narayan, S., Yee, L. D., Green, H. S., Cui, T., Zhang, Z., Baumann, K., Fort, M., Edgerton, E., Budisulistiorini, S. H., Rose, C. A., Ribeiro, I. O., e Oliveira, R. L., dos Santos, E. O., Machado, C. M. D., Szopa, S., Zhao, Y., Alves, E. G., de Sá, S. S., Hu, W., Knipping, E. M., Shaw, S. L., Junior, S. D., de Souza, R. A. F., Palm, B. B., Jimenez, J.-L., Glasius, M., Goldstein, A. H., Pye, H. O. T., Gold, A., Turpin, B. J., Vizuete, W., Martin, S. T., Thornton, J. A., Dutcher,
700   C. S., Ault, A. P., and Surratt, J. D.: Increasing Isoprene Epoxydiol-to-Inorganic Sulfate Aerosol Ratio Results in Extensive Conversion of Inorganic Sulfate to Organosulfur Forms: Implications for Aerosol Physicochemical Properties, Environmental Science Technology, 53, 8682–8694, https://doi.org/10.1021/acs.est.9b01019, 2019.

Rizzo, L. V., Roldin, P., Brito, J., Backman, J., Swietlicki, E., Krejci, R., Tunved, P., Petäjä, T., Kulmala, M., and Artaxo, P.: Multi-year statistical and modeling analysis of submicrometer aerosol number size distributions at a rain forest site in Amazonia, Atmospheric
705   Chemistry and Physics, 18, 10 255–10 274, https://doi.org/10.5194/acp-18-10255-2018, 2018.

Rollins, A. W., Kiendler-Scharr, A., Fry, J. L., Brauers, T., Brown, S. S., Dorn, H.-P., Dubé, W. P., Fuchs, H., Mensah, A., Mentel, T. F., Rohrer, F., Tillmann, R., Wegener, R., Wooldridge, P. J., and Cohen, R. C.: Isoprene oxidation by nitrate radical: alkyl nitrate and secondary organic aerosol yields, Atmospheric Chemistry and Physics, 9, 6685–6703, https://doi.org/10.5194/acp-9-6685-2009, 2009.

Rolph, G., Stein, A., and Stunder, B.: Real-time Environmental Applications and Display sYstem: READY, Environmental Modelling Soft-
710   ware, 95, 210–228, https://doi.org/10.1016/j.envsoft.2017.06.025, 2017.

Saleska, S.: AmeriFlux BASE BR-Sa1 Santarem-Km67-Primary Forest, Ver. 5-5, AmeriFlux AMP, (Dataset). Last accessed 5/22/2022, https://doi.org/https://doi.org/10.17190/AMF/1245994, 2019.

Saleska, S. R., Miller, S. D., Matross, D. M., Goulden, M. L., Wofsy, S. C., Rocha, H. R. D., Camargo, P. B. D., Crill, P., Daube, B. C., Freitas, H. C. D., Hutyra, L., Keller, M., Kirchhoff, V., Menton, M., Munger, J. W., Pyle, E. H., Rice, A. H.,

715   and Silva, H.: Carbon in Amazon Forests: Unexpected Seasonal Fluxes and Disturbance-Induced Losses, Science, 302, 1554–1557, https://doi.org/10.1126/SCIENCE.1091165/SUPPL_FILE/SALESKA.SOM.PDF, 2003.

Samaké, A., Jaffrezo, J.-L., Favez, O., Weber, S., Jacob, V., Canete, T., Albinet, A., Charron, A., Riffault, V., Perdrix, E., Waked, A., Golly, B., Salameh, D., Chevrier, F., Oliveira, D. M., Besombes, J.-L., Martins, J. M. F., Bonnaire, N., Conil, S., Guillaud, G., Mesbah, B., Rocq, B., Robic, P.-Y., Hulin, A., Meur, S. L., Descheemaecker, M., Chretien, E., Marchand, N., and Uzu, G.: Arabitol, mannitol, and glucose as
720   tracers of primary biogenic organic aerosol: the influence of environmental factors on ambient air concentrations and spatial distribution over France, Atmospheric Chemistry and Physics, 19, 11 013–11 030, https://doi.org/10.5194/acp-19-11013-2019, 2019.

Sarkar, C., Guenther, A. B., Park, J. H., Seco, R., Seco, R., Alves, E., Alves, E., Batalha, S., Santana, R., Kim, S., Smith, J., Tóta, J., and Vega, O.: PTR-TOF-MS eddy covariance measurements of isoprene and monoterpene fluxes from an eastern Amazonian rainforest, Atmospheric Chemistry and Physics, 20, 7179–7191, https://doi.org/10.5194/ACP-20-7179-2020, 2020.

725   Seinfeld, J. H. and Pandis, S. N.: Atmospheric chemistry and physics : from air pollution to climate change, Wiley, 2nd edn., 2006.

Shalamzari, M. S., Ryabtsova, O., Kahnt, A., Vermeylen, R., Hérent, M., Quetin-Leclercq, J., der Veken, P. V., Maenhaut, W., and Claeys, M.: Mass spectrometric characterization of organosulfates related to secondary organic aerosol from isoprene, Rapid Communications in Mass Spectrometry, 27, 784–794, https://doi.org/10.1002/rcm.6511, 2013.

Shrivastava, M., Andreae, M. O., Artaxo, P., Barbosa, H. M. J., Berg, L. K., Brito, J., Ching, J., Easter, R. C., Fan, J., Fast, J. D., Feng, Z.,
730   Fuentes, J. D., Glasius, M., Goldstein, A. H., Alves, E. G., Gomes, H., Gu, D., Guenther, A., Jathar, S. H., Kim, S., Liu, Y., Lou, S., Martin, S. T., McNeill, V. F., Medeiros, A., de Sá, S. S., Shilling, J. E., Springston, S. R., Souza, R. A. F., Thornton, J. A., Isaacman-VanWertz, G., Yee, L. D., Ynoue, R., Zaveri, R. A., Zelenyuk, A., and Zhao, C.: Urban pollution greatly enhances formation of natural aerosols over the Amazon rainforest, Nature Communications, 10, 1046, https://doi.org/10.1038/s41467-019-08909-4, 2019.

Sipilä, M., Berndt, T., Petäjä, T., Brus, D., Vanhanen, J., Stratmann, F., Patokoski, J., Mauldin, R. L., Hyvärinen, A.-P., Lihavainen, H., and
735   Kulmala, M.: The Role of Sulfuric Acid in Atmospheric Nucleation, Science, 327, 1243–1246, https://doi.org/10.1126/science.1180315, 2010.

Smith, J. N.: Supporting data for: Seasonal Investigation of Ultrafine Particle Composition in an Eastern Amazonian Rainforest, Dryad [data set], https://doi.org/10.5061/dryad.k6djh9wgb, 2024.

Stein, A., Draxler, R., Rolph, G., Stunder, B., Cohen, M., and Ngan, F.: NOAA's HYSPLIT Atmospheric Transport and Dispersion Modeling
740   System, Bulletin of the American Meteorological Society, 96, 2059–2077, https://doi.org/10.1175/BAMS-D-14-00110.1, 2015.

Surratt, J. D., Kroll, J. H., Kleindienst, T. E., Edney, E. O., Claeys, M., Sorooshian, A., Ng, N. L., Offenberg, J. H., Lewandowski, M., Jaoui, M., Flagan, R. C., and Seinfeld, J. H.: Evidence for Organosulfates in Secondary Organic Aerosol, Environmental Science Technology, 41, 517–527, https://doi.org/10.1021/es062081q, 2007a.

Surratt, J. D., Lewandowski, M., Offenberg, J. H., Jaoui, M., Kleindienst, T. E., Edney, E. O., and Seinfeld, J. H.: Ef-
745   fect of Acidity on Secondary Organic Aerosol Formation from Isoprene, Environmental Science Technology, 41, 5363–5369, https://doi.org/10.1021/es0704176, 2007b.

Surratt, J. D., Gómez-González, Y., Chan, A. W. H., Vermeylen, R., Shahgholi, M., Kleindienst, T. E., Edney, E. O., Offenberg, J. H., Lewandowski, M., Jaoui, M., Maenhaut, W., Claeys, M., Flagan, R. C., and Seinfeld, J. H.: Organosulfate Formation in Biogenic Secondary Organic Aerosol, The Journal of Physical Chemistry A, 112, 8345–8378, https://doi.org/10.1021/jp802310p, 2008.

750   Szmigielski, R., Surratt, J. D., Gómez-González, Y., der Veken, P. V., Kourtchev, I., Vermeylen, R., Blockhuys, F., Jaoui, M., Kleindienst, T. E., Lewandowski, M., Offenberg, J. H., Edney, E. O., Seinfeld, J. H., Maenhaut, W., and Claeys, M.: 3-methyl-

1,2,3-butanetricarboxylic acid: An atmospheric tracer for terpene secondary organic aerosol, Geophysical Research Letters, 34, https://doi.org/10.1029/2007GL031338, 2007.

Varble, A. C., Igel, A. L., Morrison, H., Grabowski, W. W., and Lebo, Z. J.: Opinion: A critical evaluation of the evidence for aerosol
755   invigoration of deep convection, Atmospheric Chemistry and Physics, 23, 13 791–13 808, https://doi.org/10.5194/acp-23-13791-2023, 2023.

Wang, J., Krejci, R., Giangrande, S., Kuang, C., Barbosa, H. M. J., Brito, J., Carbone, S., Chi, X., Comstock, J., Ditas, F., Lavric, J., Manninen, H. E., Mei, F., Moran-Zuloaga, D., Pöhlker, C., Pöhlker, M. L., Saturno, J., Schmid, B., Souza, R. A. F., Springston, S. R., Tomlinson, J. M., Toto, T., Walter, D., Wimmer, D., Smith, J. N., Kulmala, M., Machado, L. A. T., Artaxo, P., Andreae, M. O., Petäjä,
760   T., and Martin, S. T.: Amazon boundary layer aerosol concentration sustained by vertical transport during rainfall, Nature, 539, 416–419, https://doi.org/10.1038/nature19819, 2016.

Wang, M. and Penner, J. E.: Aerosol indirect forcing in a global model with particle nucleation, Atmospheric Chemistry and Physics, 9, 239–260, https://doi.org/10.5194/acp-9-239-2009, 2009.

Weigel, R., Borrmann, S., Kazil, J., Minikin, A., Stohl, A., Wilson, J. C., Reeves, J. M., Kunkel, D., de Reus, M., Frey, W., Lovejoy, E. R.,
765   Volk, C. M., Viciani, S., D'Amato, F., Schiller, C., Peter, T., Schlager, H., Cairo, F., Law, K. S., Shur, G. N., Belyaev, G. V., and Curtius, J.: In situ observations of new particle formation in the tropical upper troposphere: the role of clouds and the nucleation mechanism, Atmospheric Chemistry and Physics, 11, 9983–10 010, https://doi.org/10.5194/acp-11-9983-2011, 2011.

Westervelt, D. M., Pierce, J. R., Riipinen, I., Trivitayanurak, W., Hamed, A., Kulmala, M., Laaksonen, A., Decesari, S., and Adams, P. J.: Formation and growth of nucleated particles into cloud condensation nuclei: model–measurement comparison, Atmospheric Chemistry
770   and Physics, 13, 7645–7663, https://doi.org/10.5194/acp-13-7645-2013, 2013.

Williamson, C. J., Kupc, A., Axisa, D., Bilsback, K. R., Bui, T., Campuzano-Jost, P., Dollner, M., Froyd, K. D., Hodshire, A. L., Jimenez, J. L., Kodros, J. K., Luo, G., Murphy, D. M., Nault, B. A., Ray, E. A., Weinzierl, B., Wilson, J. C., Yu, F., Yu, P., Pierce, J. R., and Brock, C. A.: A large source of cloud condensation nuclei from new particle formation in the tropics, Nature, 574, 399–403, https://doi.org/10.1038/s41586-019-1638-9, 2019.

775   Yáñez-Serrano, A. M., Nölscher, A. C., Bourtsoukidis, E., Alves, E. G., Ganzeveld, L., Bonn, B., Wolff, S., Sa, M., Yamasoe, M., Williams, J., Andreae, M. O., and Kesselmeier, J.: Monoterpene chemical speciation in a tropical rainforest:variation with season, height, and time of dayat the Amazon Tall Tower Observatory (ATTO), Atmospheric Chemistry and Physics, 18, 3403–3418, https://doi.org/10.5194/acp-18-3403-2018, 2018.

Yáñez-Serrano, A. M., Bourtsoukidis, E., Alves, E. G., Bauwens, M., Stavrakou, T., Llusià, J., Filella, I., Guenther, A., Williams, J., Artaxo,
780   P., Sindelarova, K., Doubalova, J., Kesselmeier, J., and Peñuelas, J.: Amazonian biogenic volatile organic compounds under global change, Global Change Biology, 26, 4722–4751, https://doi.org/10.1111/gcb.15185, 2020.

Zhang, Y., Chen, Y., Lambe, A. T., Olson, N. E., Lei, Z., Craig, R. L., Zhang, Z., Gold, A., Onasch, T. B., Jayne, J. T., Worsnop, D. R., Gaston, C. J., Thornton, J. A., Vizuete, W., Ault, A. P., and Surratt, J. D.: Effect of the Aerosol-Phase State on Secondary Organic Aerosol Formation from the Reactive Uptake of Isoprene-Derived Epoxydiols (IEPOX), Environmental Science Technology Letters, 5, 167–174,
785   https://doi.org/10.1021/acs.estlett.8b00044, 2018.

Zhao, B., Shrivastava, M., Donahue, N. M., Gordon, H., Schervish, M., Shilling, J. E., Zaveri, R. A., Wang, J., Andreae, M. O., Zhao, C., Gaudet, B., Liu, Y., Fan, J., and Fast, J. D.: High concentration of ultrafine particles in the Amazon free troposphere produced by organic new particle formation, Proceedings of the National Academy of Sciences, 117, 25 344–25 351, https://doi.org/10.1073/pnas.2006716117, 2020.